

Reflective Cracking Study: First-Level Report on HVS Testing on Section 589RF — 45 mm MB4-G Overlay

Authors:

D. Jones, R Wu, J Lea and J. Harvey

Partnered Pavement Research Program (PPRC) Contract Strategic Plan Element 4.10:
Development of Improved Rehabilitation Designs for Reflective Cracking

PREPARED FOR:

California Department of Transportation
Division of Research and Innovation
Office of Roadway Research

PREPARED BY:

University of California
Pavement Research Center
UC Davis, UC Berkeley



Title: Reflective Cracking Study: First-Level Report on HVS Testing on Section 589RF - 45 mm MB4-G Overlay

Author: D. Jones, R Wu, J Lea, and J. Harvey

Prepared for:
Caltrans

FHWA No:
CA091073C

Date:
August 2006

Contract No:
65A0172

Client Reference No:
SPE 4.10

Status:
Stage 6, Approved Version

Abstract:

This report is the second in a series of first-level analysis reports that describe the results of HVS testing on a full-scale experiment being performed at the Richmond Field Station (RFS) to validate Caltrans overlay strategies for the rehabilitation of cracked asphalt concrete. It describes the results of the second HVS reflective cracking testing section, designated 589RF, carried out on a 45-mm half-thickness MB4-G overlay. The test forms part of Partnered Pavement Research Center Strategic Plan Item 4.10: "Development of Improved Rehabilitation Designs for Reflective Cracking".

HVS trafficking on the section commenced on June 23, 2004 and was completed on February 08, 2005. A total of 2,086,004 load repetitions, equating to 68.7 million ESALs and a Traffic Index of 15, was applied during this period. Temperatures were maintained at 20°C±4°C for the first one million repetitions, then at 15°C±4°C for the remainder of the test.

Findings and observations based on the data collected during this HVS study include:

- Some longitudinal cracking (1.55 m/m²), associated with severe deformation, was observed at one end of the section. Apart from this, no reflective cracking from the underlying severely cracked DGAC layer was observed on the MB4-G overlay after two million HVS repetitions. This implies that the MB4-G mix used successfully prevented reflective cracking.
- The average maximum rut depth across the entire test section at the end of the test was 37 mm, which exceeded the experiment failure criterion of 12.5 mm reached after approximately 820,000 repetitions. As no cracking was observed, the test was continued to gain a better understanding of the MB4-G overlay performance. Despite conducting HVS testing at relatively low pavement temperatures, the MB4-G overlay appeared susceptible to rutting from early in the experiment.
- Analysis of surface profile and in-depth permanent deformation measurements indicate that between 68 and 85 percent of the permanent deformation occurred in the surfacing layers with the remainder predominantly in the aggregate base layer. Negligible deformation appears to have occurred in the subgrade.

No recommendations as to the use of the modified binders in overlay mixes are made at this time. These recommendations will be included in the second-level analysis report, which will be prepared and submitted on completion of all HVS and laboratory testing.

Keywords:

Reflective cracking, overlay, modified binder, HVS test, MB Road

Proposals for implementation:

Related documents:

UCPRC-RR-2005-03, UCPRC-RR-2006-04

Signatures:

D. Jones
1st Author

J Harvey
Technical Review

D. Spinner
Editor

J. Harvey
Principal Investigator

M Samadian
Caltrans Contract Manager

DISCLAIMER

The contents of this report reflect the views of the authors who are responsible for the facts and accuracy of the data presented herein. The contents do not necessarily reflect the official views or policies of the State of California or the Federal Highway Administration. This report does not constitute a standard, specification, or regulation.

PROJECT OBJECTIVES

The objective of this project is to develop improved rehabilitation designs for reflective cracking for California.

This objective will be met after completion of four tasks identified by the Caltrans/Industry Rubber Asphalt Concrete Task Group (RACTG):

1. Develop improved mechanistic models of reflective cracking in California
2. Calibrate and verify these models using laboratory and HVS testing
3. Evaluate the most effective strategies for reflective cracking
4. Provide recommendations for reflective cracking strategies

This document is one of a series addressing Tasks 2 and 3.

ACKNOWLEDGEMENTS

The University of California Pavement Research Center acknowledges the assistance of the Rubber Pavements Association, Valero Energy Corporation, and Paramount Petroleum which contributed funds and asphalt binders for the construction of the Heavy Vehicle Simulator test track discussed in this study.

REFLECTIVE CRACKING STUDY REPORTS

The reports prepared during the reflective cracking study document data from construction, Heavy Vehicle Simulator (HVS) tests, laboratory tests, and subsequent analyses. These include a series of first- and second-level analysis reports and two summary reports. On completion of the study this suite of documents will include:

1. Reflective Cracking Study: Summary of Construction Activities, Phase 1 HVS testing and Overlay Construction (UCPRC-RR-2005-03).
2. Reflective Cracking Study: First-level Report on the HVS Rutting Experiment (UCPRC-RR-2007-06).
3. Reflective Cracking Study: First-level Report on HVS Testing on Section 590RF — 90 mm MB4-G Overlay (UCPRC-RR-2006-04).
4. Reflective Cracking Study: First-level Report on HVS Testing on Section 589RF — 45 mm MB4-G Overlay (UCPRC-RR-2006-05).
5. Reflective Cracking Study: First-level Report on HVS Testing on Section 587RF — 45 mm RAC-G Overlay (UCPRC-RR-2006-06).
6. Reflective Cracking Study: First-level Report on HVS Testing on Section 588RF — 90 mm AR4000-D Overlay (UCPRC-RR-2006-07).
7. Reflective Cracking Study: First-level Report on HVS Testing on Section 586RF — 45 mm MB15-G Overlay (UCPRC-RR-2006-12).
8. Reflective Cracking Study: First-level Report on HVS Testing on Section 591RF — 45 mm MAC15-G Overlay (UCPRC-RR-2007-04).
9. Reflective Cracking Study: HVS Test Section Forensic Report (UCPRC-RR-2007-05).
10. Reflective Cracking Study: First-level Report on Laboratory Fatigue Testing (UCPRC-RR-2006-08).
11. Reflective Cracking Study: First-level Report on Laboratory Shear Testing (UCPRC-RR-2006-11).
12. Reflective Cracking Study: Back Calculation of FWD Data from HVS Test Sections (UCPRC-RR-2007-08).
13. Reflective Cracking Study: Second-level Analysis Report (UCPRC-RR-2007-09).
14. Reflective Cracking Study: Summary Report (UCPRC-SR-2007-01). Detailed summary report.
15. Reflective Cracking Study: Summary Report (UCPRC-SR-2007-03). Four page summary report.

CONVERSION FACTORS

SI* (MODERN METRIC) CONVERSION FACTORS				
APPROXIMATE CONVERSIONS TO SI UNITS				
Symbol	Convert From	Multiply By	Convert To	Symbol
LENGTH				
in	inches	25.4	millimeters	mm
ft	feet	0.305	meters	m
AREA				
in ²	square inches	645.2	square millimeters	mm ²
ft ²	square feet	0.093	square meters	m ²
VOLUME				
ft ³	cubic feet	0.028	cubic meters	m ³
MASS				
lb	pounds	0.454	kilograms	kg
TEMPERATURE (exact degrees)				
°F	Fahrenheit	5 (F-32)/9 or (F-32)/1.8	Celsius	C
FORCE and PRESSURE or STRESS				
lbf	poundforce	4.45	newtons	N
lbf/in ²	poundforce/square inch	6.89	kilopascals	kPa
APPROXIMATE CONVERSIONS FROM SI UNITS				
Symbol	Convert From	Multiply By	Convert To	Symbol
LENGTH				
mm	millimeters	0.039	inches	in
m	meters	3.28	feet	ft
AREA				
mm ²	square millimeters	0.0016	square inches	in ²
m ²	square meters	10.764	square feet	ft ²
VOLUME				
m ³	cubic meters	35.314	cubic feet	ft ³
MASS				
kg	kilograms	2.202	pounds	lb
TEMPERATURE (exact degrees)				
C	Celsius	1.8C+32	Fahrenheit	F
FORCE and PRESSURE or STRESS				
N	newtons	0.225	poundforce	lbf
kPa	kilopascals	0.145	poundforce/square inch	lbf/in ²

*SI is the symbol for the International System of Units. Appropriate rounding should be made to comply with Section 4 of ASTM E380.
(Revised March 2003)

EXECUTIVE SUMMARY

This report is the second in a series of first-level analysis reports that describe the results of HVS testing on a full-scale experiment being performed at the Richmond Field Station (RFS) to validate Caltrans overlay strategies for the rehabilitation of cracked asphalt concrete. It describes the results of the second HVS reflective cracking testing section, designated 589RF, carried out on a 45-mm half-thickness MB4-G overlay. The testing forms part of Partnered Pavement Research Center Strategic Plan Item 4.10: “Development of Improved Rehabilitation Designs for Reflective Cracking.”

The objective of this project is to develop improved rehabilitation designs for reflective cracking for California. This objective will be met after completion of the following four tasks:

1. Develop improved mechanistic models of reflective cracking in California
2. Calibrate and verify these models using laboratory and HVS testing
3. Evaluate the most effective strategies for reflective cracking
4. Provide recommendations for reflective cracking strategies

This report is one of a series addressing Tasks 2 and 3. It consists of three main chapters. Chapter 2 provides information on the experiment layout, pavement design, HVS trafficking of the underlying layer, and the test details, including test duration, pavement instrumentation and monitoring methods, loading program, test section failure criteria, and the environmental conditions recorded over the duration of the test. Chapter 3 summarizes the data collected and includes discussion of air and pavement temperatures during testing (measured with thermocouples), elastic deflection (measured on the surface with the Road Surface Deflectometer and at depth with Multi-depth Deflectometers), permanent deformation (measured on the surface with the Laser Profilometer and at depth with Multi-depth Deflectometers), and visual inspections. Chapter 4 provides a summary and lists key findings.

The underlying pavement was designed following standard Caltrans procedures and it incorporates a 410-mm (16.1 in) Class 2 aggregate base on subgrade with a 90-mm (3.5 in) dense-graded asphalt concrete (DGAC) surface. Design thickness was based on a subgrade R-value of 5 and a Traffic Index of 7 (~121,000 equivalent standard axles, or ESALs). This structure was trafficked with the HVS in 2003 to induce fatigue cracking then overlaid with six different treatments to assess their ability to limit reflective cracking. The treatments included:

- Half-thickness (45 mm) MB4 gap-graded overlay (referred to as “45 mm MB4-G” in this report)
- Full-thickness (90 mm) MB4 gap-graded overlay (referred to as “90 mm MB4-G” in this report)

- Half-thickness MB4 gap-graded overlay with minimum 15 percent recycled tire rubber (referred to as “MB15-G” in this report)
- Half-thickness MAC15TR gap-graded overlay with minimum 15 percent recycled tire rubber (referred to as “MAC15-G” in this report)
- Half-thickness rubberized asphalt concrete gap-graded overlay (RAC-G), included as a control for performance comparison purposes (the section discussed in this report)
- Full-thickness (90 mm) AR4000 dense-graded overlay (AR4000-D), included as a control for performance comparison purposes

The thickness for the AR4000-D overlay was determined according to Caltrans Test Method 356. The other overlay thicknesses were either the same or half of the AR4000-D overlay thickness. Details on construction and the first phase of trafficking are provided in an earlier report.

A laboratory fatigue and shear study is being conducted in parallel with HVS testing. Results of these studies will be detailed in separate reports. Comparison of the laboratory and test section performance, including the results of a forensic investigation to be conducted when all testing is complete, will be discussed in a second-level report once all the data from all of the studies has been collected and analyzed.

HVS trafficking on the section commenced on June 23, 2004, and was completed on February 08, 2005. During this period a total of 2,086,004 load repetitions at loads varying between 60 kN (13,500 lb) and 100 kN (22,500 lb) were applied, which equates to approximately 68.7 million ESALs, using the Caltrans conversion of $(\text{axle load}/18,000)^{4.2}$, and to a Traffic Index of 15. A temperature chamber was used to maintain the pavement temperature at $20^{\circ}\text{C}\pm 4^{\circ}\text{C}$ ($68^{\circ}\text{F}\pm 7^{\circ}\text{F}$) for the first one million repetitions and at $15^{\circ}\text{C}\pm 4^{\circ}\text{C}$ ($59^{\circ}\text{F}\pm 7^{\circ}\text{F}$) for the remainder of the test. A dual tire (720 kPa [104 psi] pressure) and bidirectional loading with lateral wander was used.

Findings and observations based on the data collected during this HVS study include:

- Cracking was observed at one end of the section where significant deformation (rutting and shoving) had occurred. It was first recorded after 1.5 million repetitions and no further cracking was noted after about 1.6 million repetitions. On completion of testing, the crack density was 1.55 m/m^2 (0.47 ft/ft^2), considerably lower than the failure criterion of 2.5 m/m^2 (0.76 ft/ft^2) set for the experiment. The cracks were predominantly longitudinal and cracking patterns did not correspond with those in the underlying DGAC layer. Apart from the cracks associated with deformation at the end of the section, the MB4-G overlay appeared to successfully prevent any

cracking in the underlying layer from reflecting through to the surface, despite final-to-initial deflections indicating that considerable damage had occurred in the asphalt layers.

- The average maximum rut depth across the entire test section at the end of the test was 37.2 mm (1.46 in) which exceeded the Caltrans (and experiment) failure criterion of 12.5 mm (0.5 in) reached after approximately 820,000 repetitions. At this point, no cracking was observed and the test was therefore continued to gain a better understanding of the MB4-G overlay performance. The maximum rut depth measured on the section was 106 mm (4.17 in). Despite conducting HVS testing at relatively low pavement temperatures ($20^{\circ}\text{C}\pm 4^{\circ}\text{C}$ [$68^{\circ}\text{F}\pm 7^{\circ}\text{F}$]) for the first one million repetitions and $15^{\circ}\text{C}\pm 4^{\circ}\text{C}$ [$59^{\circ}\text{F}\pm 7^{\circ}\text{F}$] for the remainder of the test, the MB4-G overlay appeared susceptible to rutting from early in the experiment.
- Ratios of final-to-initial elastic surface deflections under a 60 kN (13,500 lb) wheel load increased by between 2.1 and 2.9 times along the length of the section. The ratios for in-depth deflections show that damage had increased significantly at all depths in the pavement structure by the end of trafficking. Loss of stiffness was highest in the area of most severe cracking in the underlying DGAC layer.
- Analysis of surface profile and in-depth permanent deformation measurements indicate that most of the permanent deformation (between 68 and 86 percent along the length of the section) occurred in the asphalt-bound surfacing layers (overlay and cracked DGAC) with the remainder in the aggregate base layer. Some deformation occurred in the subgrade below the point of greatest maximum rut. Contribution to total permanent deformation at this point was 68, 26, and 6 percent for the surfacing, aggregate base, and subgrade respectively.

No recommendations as to the use of modified binders in overlay mixes are made at this time. These recommendations will be included in the second-level analysis report, which will be prepared and submitted on completion of all HVS and laboratory testing.

TABLE OF CONTENTS

EXECUTIVE SUMMARY	v
LIST OF TABLES	xi
LIST OF FIGURES	xii
1. INTRODUCTION	1
1.1. Objectives	1
1.2. Overall Project Organization	1
1.3. Structure and Content of This Report.....	4
1.4. Measurement Units.....	4
2. TEST DETAILS	5
2.1. Experiment Layout	5
2.2. Test Section Layout	5
2.2.1 Pavement Instrumentation and Monitoring Methods.....	8
2.3. Underlying Pavement Design	8
2.4. Summary of Testing on the Underlying Layer	9
2.5. Reflective Cracking Section Design.....	10
2.6. Test Summary.....	11
2.6.1 Test Section Failure Criteria.....	11
2.6.2 Environmental Conditions.....	11
2.6.3 Test Duration.....	12
2.6.4 Loading Program.....	12
2.6.5 Measurement Summary.....	13
3. DATA SUMMARY	17
3.1. Temperatures	17
3.1.1 Air Temperatures in the Temperature Control Unit.....	17
3.1.2 Outside Air Temperatures	19
3.1.3 Temperature in the Asphalt Concrete Layer	19
3.2. Rainfall	20
3.3. Elastic Deflection	20
3.3.1 Surface Elastic Deflection Using RSD.....	22
3.3.2 Surface Elastic Deflection Using FWD.....	27
3.3.3 In-depth Elastic Deflection.....	30
3.4. Permanent Deformation.....	34
3.4.1 Permanent Surface Deformation (Rutting).....	34

3.4.2	Permanent In-depth Deformation	40
3.5.	Visual Inspection	44
3.6.	Forensic Evaluation	46
3.7.	Second-level Analysis	46
4.	CONCLUSIONS	47
5.	REFERENCES.....	51

LIST OF TABLES

Table 2.1: Summary of Load History.....	12
Table 2.2: Summary of MDD and RSD Measurements.....	15
Table 2.3: Summary of FWD Measurements.....	14
Table 3.1: Temperature Summary for Air and Pavement	19
Table 3.2: Average 60 kN RSD Centerline Deflections Before and After Testing.....	22
Table 3.3: Summary of FWD Measurements.....	27
Table 3.4: Summary of 60 kN In-depth Elastic Deflections	31
Table 3.5: Vertical Permanent Deformation in Pavement Layers.....	40

LIST OF FIGURES

Figure 1.1: Timeline for the Reflective Cracking Study.	3
Figure 2.1: Layout of Reflective Cracking Study project.	6
Figure 2.2: Section 589RF layout and location of instruments.	7
Figure 2.2: Pavement design for the Reflective Cracking Study test track.....	8
Figure 2.3: Cracking pattern on Section 571RF after Phase I HVS testing.	9
Figure 2.4: Actual vs. target gradation for MB4-G overlay.	11
Figure 2.5: Cumulative traffic applications and loading history.	13
Figure 3.1: Frequencies of recorded temperatures.	18
Figure 3.2: Daily average air temperatures inside the temperature control chamber.	18
Figure 3.3: Daily average air temperatures outside the temperature control chamber.	19
Figure 3.4: Daily average temperatures at pavement surface and various depths.....	20
Figure 3.5: Monthly rainfall for Richmond Field Station.	21
Figure 3.6: RSD deflections at CL locations with 60 kN test load at test start.	23
Figure 3.7: RSD deflections at CL locations with 60 kN test load after 215,000 repetitions.	23
Figure 3.8: RSD deflections at CL locations with 60 kN test load after 407,197 repetitions.	24
Figure 3.9: RSD deflections at CL locations with 60 kN test load after 1,002,000 repetitions.	24
Figure 3.10: RSD deflections at CL locations with 60 kN test load at test completion.	25
Figure 3.11: Average RSD surface deflections with 60 kN test load (centerline and sides).....	26
Figure 3.12: Average RSD surface deflections with 60 kN test load (centerline and subsection).	26
Figure 3.13: Composite pavement stiffness (FWD Sensor 1) on section centerline.	28
Figure 3.14: Subgrade pavement stiffness (FWD Sensor 6) on section centerline.	29
Figure 3.15: Composite pavement stiffness (FWD Sensor 1) outside trafficked area.	29
Figure 3.16: Subgrade pavement stiffness (FWD Sensor 6) outside trafficked area.....	30
Figure 3.17: Elastic deflections at MDD4 with 60 kN test load.....	31
Figure 3.18: Elastic deflections at MDD8 with 60 kN test load.....	32
Figure 3.19: Elastic deflections at MDD12 with 60 kN test load.....	32
Figure 3.20: Illustration of maximum rut depth and average deformation of a leveled profile.	34
Figure 3.21: Laser profilometer cross section at various stages of trafficking.....	35
Figure 3.22: Average deformation determined from Laser Profilometer data.	36
Figure 3.23: Average maximum rut determined from Laser Profilometer data.	36
Figure 3.24: Contour plot of permanent deformation after 215,000 repetitions.	37
Figure 3.25: Contour plot of permanent deformation after 407,000 repetitions.	37
Figure 3.26: Contour plot of permanent deformation after 1,002,000 repetitions.	38

Figure 3.27: Contour plot of permanent deformation after 1,500,000 repetitions. 38

Figure 3.28: Contour plot of permanent deformation at end of test. 39

Figure 3.29: Comparison of cracking pattern from Phase 1 and rutting in Phase 2. 39

Figure 3.30: In-depth permanent deformation at MDD4. 41

Figure 3.31: In-depth differential permanent deformation of various layers at MDD4. 41

Figure 3.32: In-depth permanent deformation at MDD8. 42

Figure 3.33: In-depth differential permanent deformation of various layers at MDD8. 42

Figure 3.34: In-depth permanent deformation at MDD12. 43

Figure 3.35: In-depth differential permanent deformation of various layers at MDD12. 43

Figure 3.36: Surface cracks marked with crayon between Stations 12 and 14 at end of test. 45

Figure 3.37: Cracking pattern and pattern comparison between underlying layer and overlay. 46

1. INTRODUCTION

1.1. Objectives

The first-level analysis presented in this report is part of Partnered Pavement Research Center Strategic Plan Element 4.10 (PPRC SPE 4.10) being undertaken for the California Department of Transportation (Caltrans) by the University of California Pavement Research Center (UCPRC). The objective of the study is to evaluate the reflective cracking performance of asphalt binder mixes used in overlays for rehabilitating cracked asphalt concrete pavements in California. The study includes mixes modified with rubber and polymers, and it will develop tests, analysis methods, and design procedures for mitigating reflective cracking in overlays. This work is part of a larger study on modified binder (MB) mixes being carried out under the guidance of the Caltrans Pavement Standards Team (PST) (1), which includes laboratory and accelerated pavement testing using the Heavy Vehicle Simulator (carried out by the UCPRC), and the construction and monitoring of field test sections (carried out by Caltrans).

1.2. Overall Project Organization

This UCPRC project is a comprehensive study, carried out in three phases, involving the following primary elements (2):

- Phase 1
 - The construction of a test pavement and subsequent overlays;
 - Six separate Heavy Vehicle Simulator (HVS) tests to crack the pavement structure;
 - Placing of six different overlays on the cracked pavement;
- Phase 2
 - Six HVS tests to assess the susceptibility of the overlays to high-temperature rutting (Phase 2a);
 - Six HVS tests to determine the low-temperature reflective cracking performance of the overlays (Phase 2b);
 - Laboratory shear and fatigue testing of the various hot-mix asphalts (Phase 2c);
 - Falling Weight Deflectometer (FWD) testing of the test pavement before and after construction and before and after each HVS test;
 - Forensic evaluation of each HVS test section;
- Phase 3
 - Performance modeling and simulation of the various mixes using models calibrated with data from the primary elements listed above.

Phase 1

In this phase, a conventional dense-graded asphalt concrete (DGAC) test pavement was constructed at the Richmond Field Station (RFS) in the summer of 2001. The pavement was divided into six cells, and within each cell a section of the pavement was trafficked with the HVS until the pavement failed by either fatigue (2.5 m/m^2 [0.76 ft/ft²]) or rutting (12.5 mm [0.5 in]). This period of testing began in the summer of 2001 and was concluded in the spring of 2003. In June 2003 each test cell was overlaid with either conventional DGAC or asphalt concrete with modified binders as follows:

- Full-thickness (90 mm) AR4000-D dense graded asphalt concrete overlay, included as a control for performance comparison purposes (AR-4000 is approximately equivalent to a PG64-16 performance grade binder);
- Full-thickness (90 mm) MB4-G gap-graded overlay;
- Half-thickness (45 mm) rubberized asphalt concrete gap-graded overlay (RAC-G), included as a control for performance comparison purposes;
- Half-thickness (45 mm) MB4-G gap-graded overlay;
- Half-thickness (45 mm) MB4-G gap-graded overlay with minimum 15 percent recycled tire rubber (MB15-G), and
- Half-thickness (45 mm) MAC15-G gap-graded overlay with minimum 15 percent recycled tire rubber.

The conventional overlay was designed using the current (2003) Caltrans overlay design process. The various modified overlays were either full (90 mm) or half thickness (45 mm). Mixes were designed by Caltrans. The overlays were constructed in one day.

Phase 2

Phase 2 included high-temperature rutting and low-temperature reflective cracking testing with the HVS as well as laboratory shear and fatigue testing. The rutting tests were started and completed in the fall of 2003. For these tests, the HVS was placed above a section of the underlying pavement that had not been trafficked during Phase 1. A reflective cracking test was next conducted on each overlay from the winter of 2003-2004 to the summer of 2007. For these tests, the HVS was positioned precisely on top of the sections of failed pavement from the Phase 1 HVS tests to investigate the extent and rate of crack propagation through the overlay.

In conjunction with Phase 2 HVS testing, a full suite of laboratory testing, including shear and fatigue testing, was carried out on field-mixed, field-compacted, field-mixed, laboratory-compacted, and laboratory-mixed, laboratory-compacted specimens.

Phase 3

Phase 3 entailed a second-level analysis carried out on completion of HVS and laboratory testing (the focus of this report). This included extensive analysis and characterization of the mix fatigue and mix shear data, backcalculation of the FWD data, performance modeling of each HVS test, and a detailed series of pavement simulations carried out using the combined data.

An overview of the project timeline is shown in Figure 1.1.

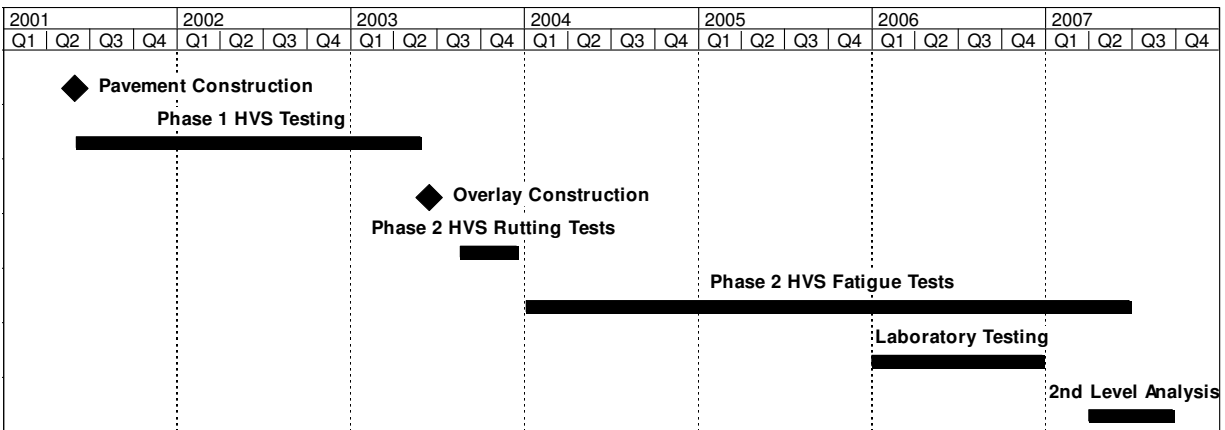


Figure 1.1: Timeline for the Reflective Cracking Study.

Reports

The reports prepared during the reflective cracking study document data from construction, HVS tests, laboratory tests, and subsequent analyses. These include a series of first- and second-level analysis reports and two summary reports. On completion of the study this suite of documents will include:

- One first-level report covering the initial pavement construction, the six initial HVS tests, and the overlay construction (Phase 1);
- One first-level report covering the six Phase 2 rutting tests (but offering no detailed explanations or conclusions on the performance of the pavements);
- Six first-level reports, each of which covers a single Phase 2 reflective cracking test (containing summaries and trends of the measured environmental conditions, pavement responses, and pavement performance but offering no detailed explanations or conclusions on the performance of the pavement);
- One first-level report covering laboratory shear testing;
- One first-level report covering laboratory fatigue testing;
- One report summarizing the HVS test section forensic investigation;
- One report summarizing the backcalculation analysis of deflection tests,

- One second-level analysis report detailing the characterization of shear and fatigue data, pavement modeling analysis, comparisons of the various overlays, and simulations using various scenarios (Phase 3), and
- One four-page summary report capturing the conclusions and one longer, more detailed summary report that covers the findings and conclusions from the research conducted by the UCPRC.

1.3. Structure and Content of This Report

This report presents the results of the HVS test on the half-thickness (45 mm) MB4 gap-graded asphalt concrete overlay (referred to as “45 mm MB45-G” in this report), designated Section 589RF, with preliminary analyses relative to observed performance and is organized as follows:

- Chapter 2 contains a description of the test program including experiment layout, loading sequence, instrumentation, and data collection.
- Chapter 3 presents a summary and discussion of the data collected during the test.
- Chapter 4 contains a summary of the results together with conclusions and observations.

1.4. Measurement Units

Metric units have always been used in the design and layout of HVS test tracks, and for all the measurements, data storage, analysis, and reporting at the eight HVS facilities worldwide (as well as all other international accelerated pavement testing facilities). Continued use of the metric system facilitates consistency in analysis, reporting, and data sharing.

In this report, metric and English units are provided in the Executive Summary, Chapters 1 and 2, and the Conclusion. In keeping with convention, only metric units are used in Chapter 3. A conversion table is provided on Page iv at the beginning of this report.

2. TEST DETAILS

2.1. Experiment Layout

Six overlays, each with a rutting test section and a reflective cracking test section, were constructed as part of the second phase of the study as follows:

1. Sections 580RF and 586RF: Half-thickness (45 mm) MB4 gap-graded overlay with minimum 15 percent recycled tire rubber (referred to as “MB15-G” in this report);
2. Sections 581RF and 587RF: Half-thickness (45 mm) rubberized asphalt concrete gap-graded (RAC-G) overlay;
3. Sections 582RF and 588RF: Full-thickness (90 mm) AR4000 dense-graded asphalt concrete overlay (designed using CTM356 and referred to as “AR4000-D” in this report);
4. Sections 583RF and 589RF: Half-thickness (45 mm) MB4 gap-graded overlay (referred to as “45 mm MB4-G” in this report);
5. Sections 584RF and 590RF: Full-thickness (90 mm) MB4 gap-graded overlay (referred to as “90 mm MB4-G” in this report), and
6. Sections 585RF and 591RF: Half-thickness (45 mm) MAC15TR gap-graded overlay with minimum 15 percent recycled tire rubber (referred to as “MAC15-G” in this report).

These sections and the corresponding Phase 1 fatigue test sections are shown in Figure 2.1. Prior to the Phase 2 reflective cracking testing, a rutting study was carried out whereby HVS loading at high temperature was applied adjacent to the reflective cracking experiments to evaluate the rutting behavior of the overlay mixes. The rutting study will be discussed in a separate report.

2.2. Test Section Layout

The test section layout for Section 591RF is shown in Figure 2.2. Station numbers refer to fixed points on the test section and are used for measurements and as a reference for discussing performance.

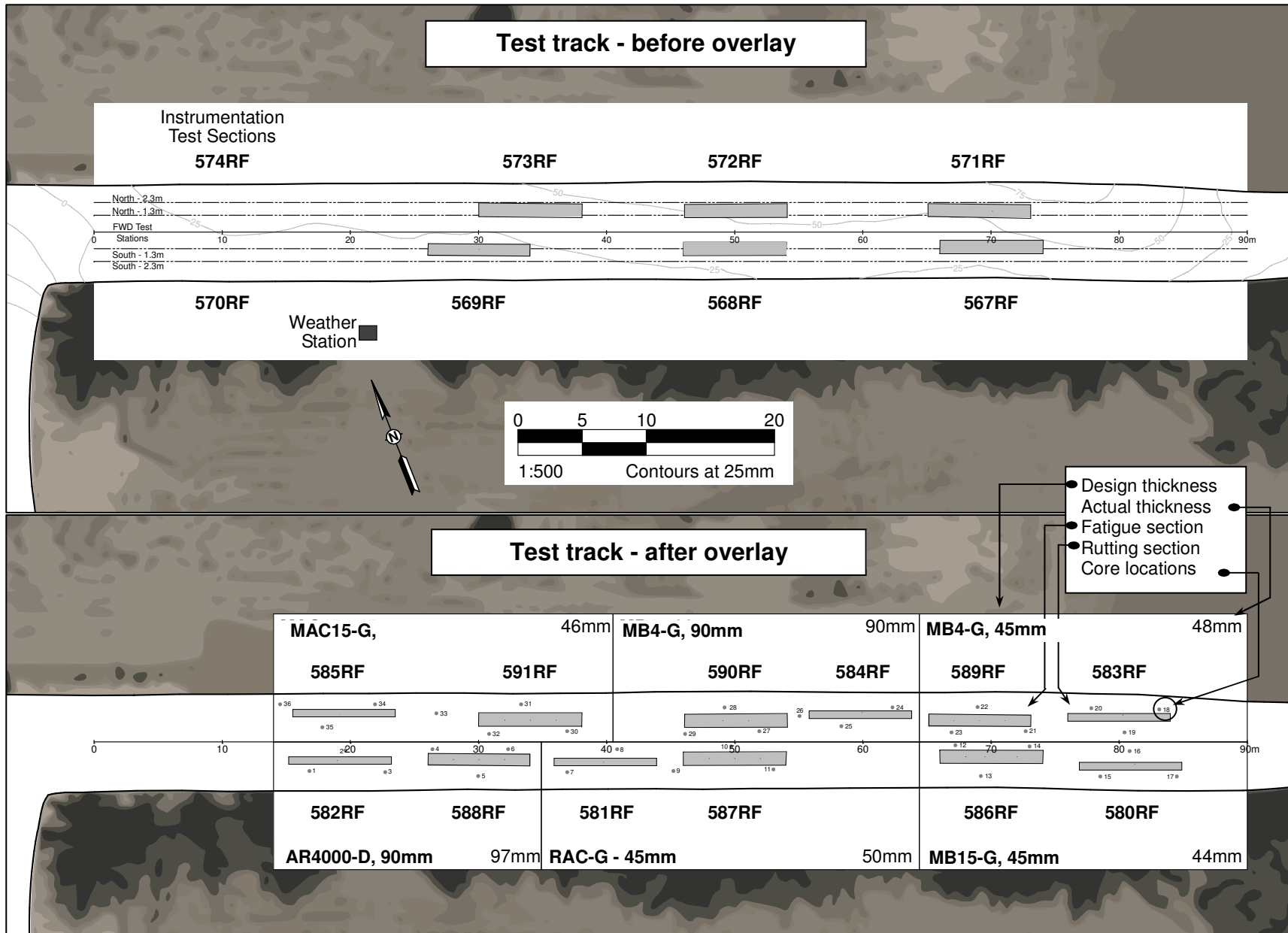
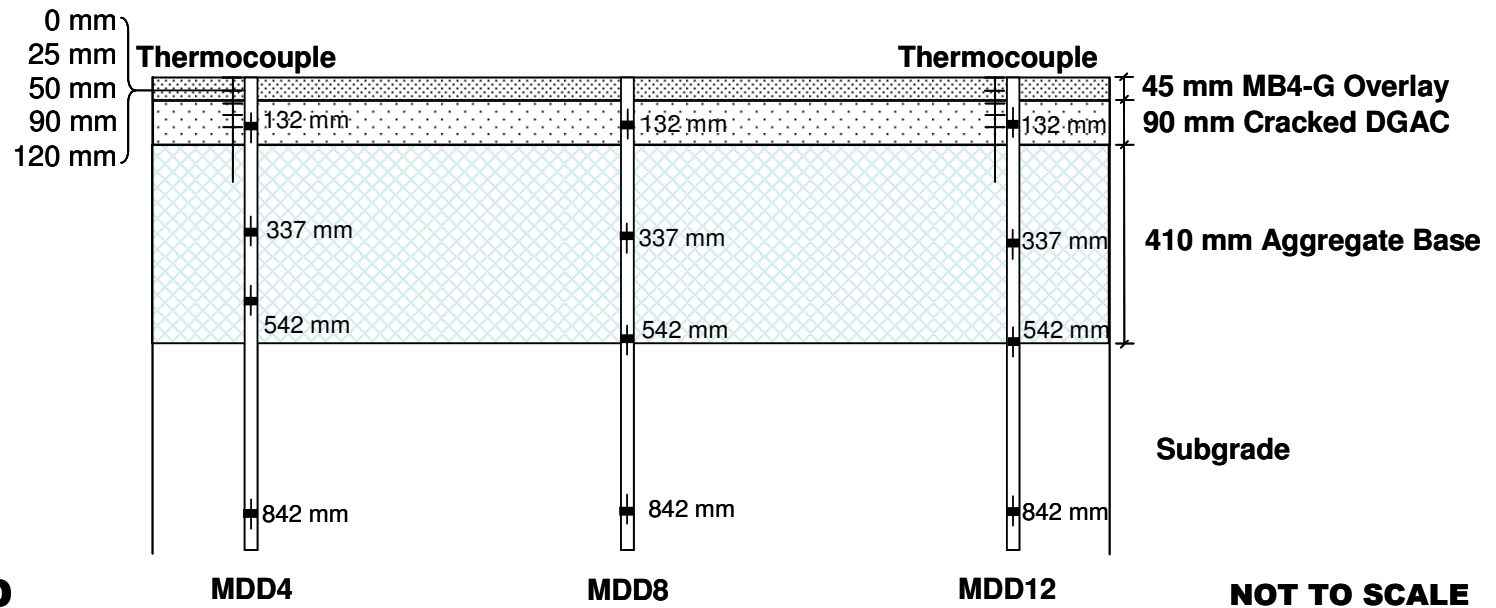
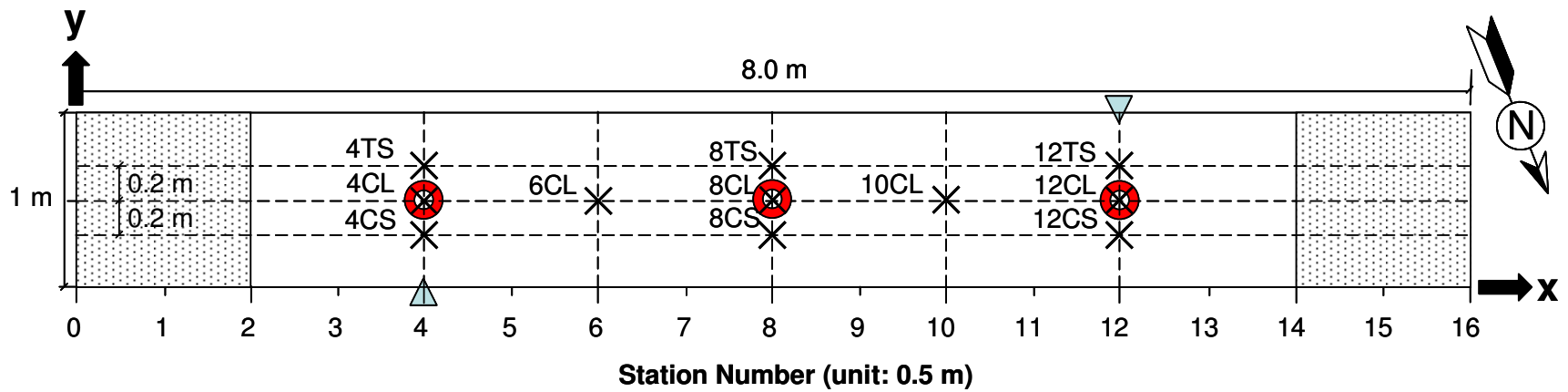


Figure 2.1: Layout of Reflective Cracking Study project.



LEGEND

	MDD		RSD		Thermocouple		MDD LVDT module	TS	Traffic Side	CL	Central Line	CS	Caravan Side
(MDD – Multi-depth Deflectometer, RSD – Road Surface Deflectometer, LVDT – Linear Variable Displacement Transducer)													

Figure 2.2: Section 589RF layout and location of instruments.

2.2.1 Pavement Instrumentation and Monitoring Methods

Measurements were taken with the following instruments:

- Road Surface Deflectometer (RSD), measuring surface deflection;
- Multi-depth Deflectometer (MDD), measuring elastic deflection and permanent deformation at different depths in the pavement;
- Laser Profilometer, measuring surface profile (at each station);
- Falling Weight Deflectometer (FWD), measuring elastic deflection before and after testing, and
- Thermocouples, measuring pavement temperature and ambient temperature.

Instrument positions are shown in Figure 2.2. Detailed descriptions of the instrumentation and measuring equipment are included in Reference 4. Intervals between measurements, in terms of load repetitions, were selected to enable adequate characterization of the pavement as damage developed.

2.3. Underlying Pavement Design

The pavement for the first phase of HVS trafficking was designed according to the Caltrans Highway Design Manual Chapter 600 using the computer program *NEWCON90*. Design thickness was based on a tested subgrade R-value of 5 and a Traffic Index of 7 (~121,000 ESALs) (3). The pavement design for the test road and the preliminary as-built pavement structure for Section 589RF (determined from cores removed from the edge of the section) are illustrated in Figure 2.3.

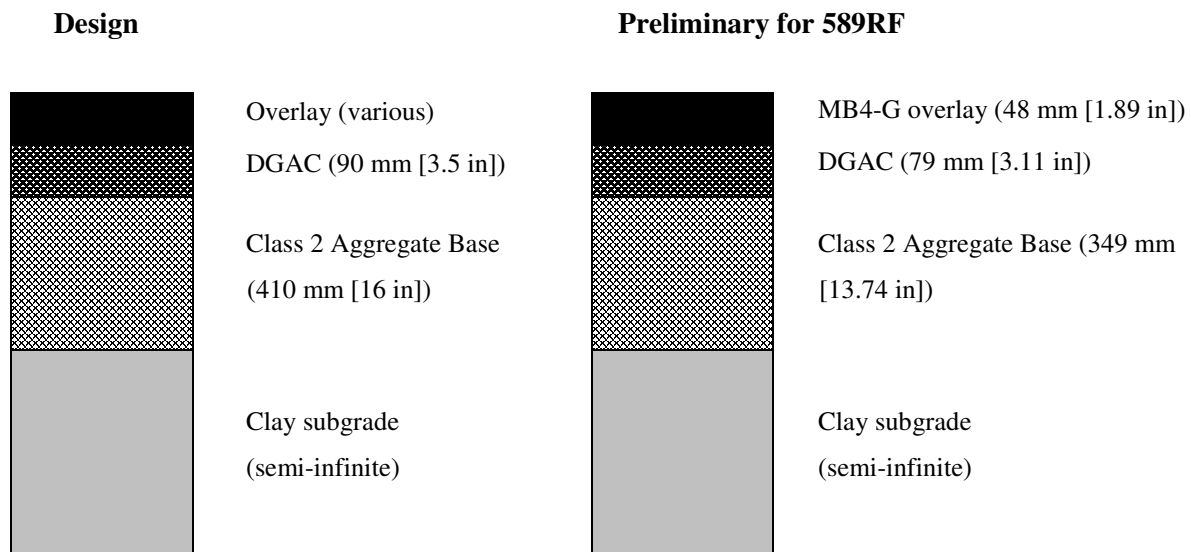


Figure 2.2: Pavement design for the Reflective Cracking Study test track
(Design and preliminary actual for 589RF)

The existing subgrade was ripped and reworked to a depth of 200 mm (8 in) so that the optimum moisture content and the maximum wet density met the specification per Caltrans Test Method CTM 216. The average maximum wet density of the subgrade was 2,180 kg/m³ (136 pcf). The average relative compaction of the subgrade was 97 percent (3).

The aggregate base was constructed to meet the Caltrans compaction requirements for aggregate base Class 2 using CTM 231 nuclear density testing. The maximum wet density of the base determined according to CTM 216 was 2,200 kg/m³ (137 pcf). The average relative compaction was 98 percent.

The DGAC layer consisted of a dense-graded asphalt concrete (DGAC) with AR-4000 binder and aggregate gradation limits following Caltrans 19-mm (0.75 in) maximum size coarse gradation (3). The target asphalt content was 5.0 percent by mass of aggregate, while actual contents varied between 4.34 and 5.69 percent. Nuclear density measurements and extracted cores were used to determine a preliminary as-built mean air-void content of 9.1 percent with a standard deviation of 1.8 percent. The air-void content after traffic compaction and additional air-void contents from cores taken outside the trafficked area will be determined on completion of trafficking of all sections and will be reported in the second-level analysis report.

2.4. Summary of Testing on the Underlying Layer

Trafficking of the underlying Section 571RF took place between July 12, 2002, and October 02, 2002, during which 1,101,553 repetitions were applied. Figure 2.3 presents the final cracking pattern after testing. Cracking was mostly transverse. Total crack length was 37.87 m (124.25 ft) and crack density was 5.41 m/m² (1.65 ft/ft²).

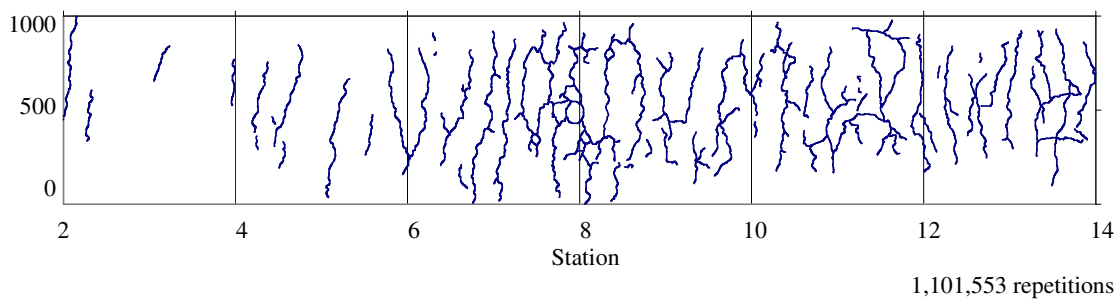


Figure 2.3: Cracking pattern on Section 571RF after Phase I HVS testing.

2.5. Reflective Cracking Section Design

Section 589RF consisted of a 45-mm MB4 gap-graded overlay constructed precisely on top of Section 571RF. Section 571RF had considerable transverse and alligator cracking over most of the area subjected to HVS trafficking (Figure 2.3), with a lower density of cracking between Stations 0 and 6, compared to between Stations 6 and 16. The overlay thickness for the experiment was determined according to Caltrans Test Method CTM 356 using Falling Weight Deflectometer data from the Phase 1 experiment. The actual layer thickness of Section 589RF was measured from cores extracted from the edge of the test section and from Dynamic Cone Penetrometer (DCP) tests. The measured average thicknesses for the section from cores and DCP measurements taken outside the trafficked area were:

- MB4-G overlay: 48 mm (min 42 mm; max 54 mm; standard deviation, 4.5 mm)
[1.9 in (min 1.7 in; max 2.1 in; standard deviation, 0.2 in)]
- Cracked DGAC layer: 78 mm (min 64 mm; max 94 mm; standard deviation, 12.2 mm)
[3.1 in (min 2.5 in; max 3.7 in; standard deviation, 0.5 in)]
- Aggregate base: 349 mm (13.7 in)

Exact layer thicknesses will be determined from measurements in test pits after HVS testing has been completed on all sections.

Laboratory testing was carried out by Caltrans and UCPRC on samples collected during construction to determine actual binder properties, binder content, aggregate gradation, and air-void content. The MB4 binder met the Caltrans MB4 modified binder specification, based on testing performed by Caltrans. The ignition-extracted binder content, corrected for aggregate ignition, showed an average value of 7.77 percent, somewhat higher than the design binder content of 7.2 percent. The aggregate gradation met Caltrans specifications for a 19.0 mm (3/4 in) maximum size gap gradation, with material passing the 6.35 mm (1/4 in) and 9.5 mm (3/8 in) sieves on the limit for course gradation. Gradation is illustrated in Figure 2.4. The preliminary as-built air-void content was 6.5 percent with a standard deviation of 0.6 percent, based on cores taken outside of the HVS sections. Final air-void contents will be determined from trenching and coring to be performed after trafficking of all sections.

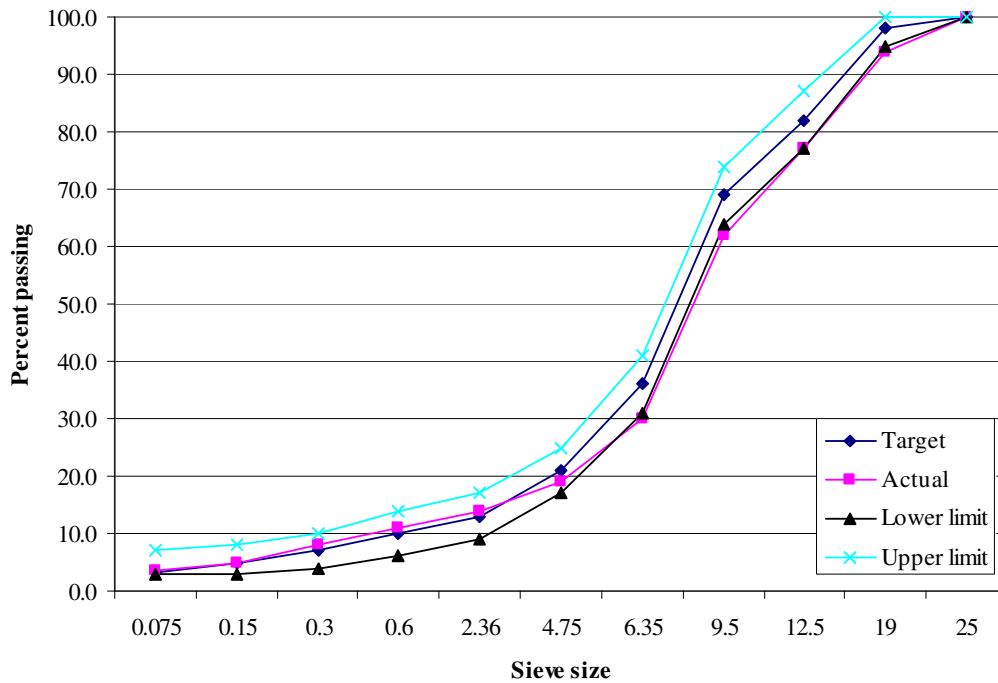


Figure 2.4: Actual vs. target gradation for MB4-G overlay.

2.6. Test Summary

2.6.1 Test Section Failure Criteria

Failure criteria for analyses were set at:

- Cracking density of 2.5 m/m^2 (0.76 ft/ft^2) or more, and/or
- Average maximum surface rut depth of 12.5 mm (0.5 in) or more.

2.6.2 Environmental Conditions

For the first one million repetitions, the pavement surface temperature was maintained at $20^\circ\text{C} \pm 4^\circ\text{C}$ ($68^\circ\text{F} \pm 7^\circ\text{F}$) to minimize rutting in the asphalt concrete and to promote fatigue damage. Thereafter, the pavement surface temperature was reduced to $15^\circ\text{C} \pm 4^\circ\text{C}$ ($59^\circ\text{F} \pm 7^\circ\text{F}$) to further accelerate fatigue damage. A temperature control chamber (5) was used to maintain the test temperatures.

The pavement surface received no direct rainfall as it was protected by the temperature control chamber. The section was tested during both dry and wet seasons (June to February) and hence water could have infiltrated the pavement from the side drains and through the raised groundwater table.

2.6.3 Test Duration

HVS trafficking of Section 589RF was initiated on June 23, 2004, and completed on February 8, 2005, after the application of over two million (2,086,004) load repetitions. Testing was interrupted twice:

- During a breakdown between October 13 and November 29, 2004, when the cumulative traffic repetitions were approximately 1.2 million, and
- For the scheduled holiday shutdown between December 24, 2004 and January 04, 2005, when the repetition count was 1,575,000.

2.6.4 Loading Program

The HVS test program is summarized in Table 2.1.

Table 2.1: Summary of Load History

Start Date	Start Repetition	Wheel Load (kN) - [lb]		Wheel	Tire Pressure (kPa) - [psi]	Direction
		Planned	Actual			
06/23/04	0	40 - [9,000]	60	Dual	720 - [104]	Bi
07/14/04	215,000	60 - [13,500]	90	Dual	720 - [104]	Bi
07/28/04	407,197	80 - [18,000]	80	Dual	720 - [104]	Bi
09/20/04*	1,002,000	100 - [22,500]	100	Dual	720 - [104]	Bi

* Testing was interrupted during a breakdown between 10/13/04 and 11/29/04 and the holiday shutdown between 12/24/04 and 01/04/05.

The loading program followed differs from the original test plan due to an incorrect hydraulic control system setup on loads less than 65 kN (14,600 lb) in the Phase 1 experiment. The loading pattern from the Phase 1 experiment was thus retained to facilitate comparisons of performance between all tests in the Reflective Cracking Study. Testing was undertaken with a dual-wheel configuration, using radial truck tires (Goodyear G159 - 11R22.5 - steel belt radial) inflated to a pressure of 720 kPa (104 psi), in a bidirectional loading mode. Lateral wander over the one-meter (39.4 in) width of the test section was programmed to simulate traffic wander on a typical highway lane.

Cumulative traffic applications and the loading history are shown in Figure 2.5. The shorter 60 kN (13,500 lb) and 90 kN (20,250 lb) and longer 80 kN (18,000 lb) and 100 kN (22,500 lb) loading phases adopted for Section 589 (second HVS test) were also used in this test. A total of 2,086,004 load repetitions were applied consisting of:

- 215,000 repetitions of a 60 kN (13,500 lb) load
- 192,197 repetitions of a 90 kN (20,250 lb) load
- 594,803 repetitions of an 80 kN (18,000 lb) load, and
- 1,084,004 repetitions of a 100 kN (22,500 lb) load.

This loading equates to approximately 68.7 million equivalent standard axles, using the Caltrans conversion of $(\text{axle load}/18000)^{4.2}$, which in turn equates to a Traffic Index of 15.

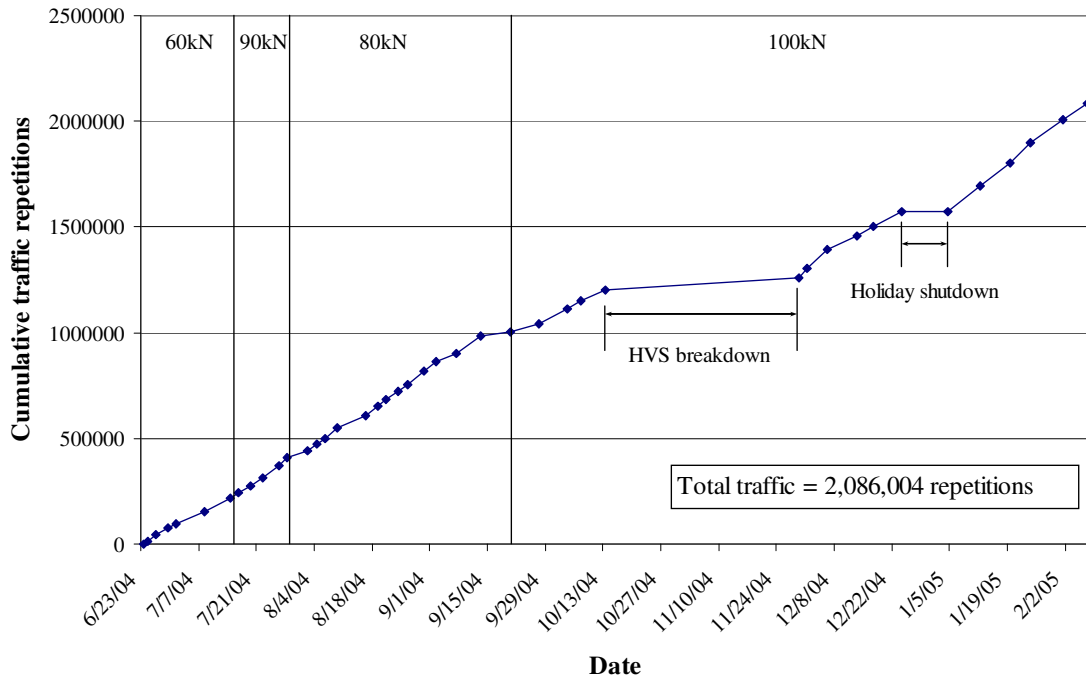


Figure 2.5: Cumulative traffic applications and loading history.

2.6.5 Measurement Summary

Table 2.2 (pages 15 and 16) lists the reading schedule of MDD and RSD measurements at various wheel loads. Surface deflection measurements with the RSD were obtained at the reference points along the centerline (CL) of the section and at locations 200 mm (8.0 in) on either side of the centerline (traffic and caravan side), as shown in Figure 2.2. MDD and RSD measurements were taken with a 60 kN (13,500 lb) load throughout the test as well as with the load being applied at the time of measurement (i.e., 80 kN [18,000 lb], 90 kN [22,500 lb], or 100 kN [22,500 lb]). The figures in Chapter 3 only show the measurements taken with the 60 kN (13,500 lb) load.

Measurements of surface rut depth taken by transverse scans with the Laser Profilometer were obtained at each station (Figure 2.2) on the same schedule as that of the MDD and RSD. The following rut parameters, which are discussed in more detail in Chapter 3, were determined from these measurements:

- Location and magnitude of the maximum rut depth,
- Average rut depth for the entire test section, and
- Rate of rut development.

Falling Weight Deflectometer (FWD) measurements were taken before and after testing at the center of and on the outside of the trafficked area. A summary of the measurement schedule is provided in Table 2.3.

Table 2.3: Summary of FWD Measurements

Date	Time	Location	Interval (m) - [ft]
06/21/04	09:36	Center & side	0.3 - [1.0]
06/21/04	10:42	Center & side	0.3 - [1.0]
02/18/05	07:30	Center & side	0.3 - [1.0]
02/24/05	15:14	Center & side	0.9 - [3.0]

Pavement temperature measurements were derived from thermocouples (depths and surface locations shown in Figure 2.2) at one-hour intervals during HVS operation. Air temperatures were measured in a weather station next to the test section and recorded at the same intervals as the thermocouples.

Crack development was monitored using visual inspection of the road surface and photographs.

Table 2.2: Summary of MDD and RSD Measurements

Date	Reps (x1million)	MDD4				MDD8				MDD12				RSD Center line ¹				RSD Sides ²			
		60*	90	80	100	60	90	80	100	60	90	80	100	60	90	80	100	60	90	80	100
06/23/04	0.00	✓				✓				✓				✓				✓			
06/26/04	0.02	✓				✓				✓				✓							
06/29/04	0.05	✓				✓				✓				✓							
7/01/04	0.08	✓				✓				✓				✓							
07/08/04	0.10	✓				✓				✓				✓							
07/14/04	0.15	✓	✓			✓	✓			✓	✓			✓	✓			✓	✓		
07/16/04	0.22	✓	✓			✓	✓			✓	✓			✓	✓						
07/19/04	0.25	✓	✓			✓	✓			✓	✓			✓	✓						
07/22/04	0.28	✓	✓			✓	✓			✓	✓			✓	✓						
07/26/04	0.31	✓	✓			✓	✓			✓	✓			✓	✓						
07/28/04	0.37	✓	✓	✓		✓	✓	✓		✓	✓	✓		✓	✓	✓		✓	✓	✓	
08/02/04	0.41	✓		✓		✓		✓		✓		✓		✓		✓					
08/04/04	0.44	✓		✓		✓		✓		✓		✓		✓		✓					
08/06/04	0.47	✓		✓		✓		✓		x		x		✓		✓					
08/09/04	0.50	✓		✓		✓		✓		✓		✓		✓		✓					
08/16/04	0.55	✓		✓		✓		✓		✓		✓		✓		✓					
08/19/04	0.61	✓	✓	✓	✓	✓	✓	✓	✓	✓	✓	✓	✓	✓	✓	✓	✓	✓	✓	✓	✓
08/21/04	0.65	✓		x	✓	✓		x	✓	✓		x	✓	✓		x	✓				
08/24/04	0.69	✓		x	✓	✓		x	✓	✓		x	✓	✓		x	✓				
08/26/04	0.72	✓		✓	x	✓		✓	x	✓		✓	x	✓		✓	x				
08/30/04	0.76	✓		✓	x	✓		✓	x	✓		✓	x	✓		✓	x				
09/02/04	0.82	✓		✓	x	✓		✓	x	✓		✓	x	✓		✓	x				
09/07/04	0.86	✓		✓	x	✓		✓	x	✓		✓	x	✓		✓	x				
09/13/04	0.90	✓		✓	x	✓		✓	x	✓		✓	x	✓		✓	x				
09/20/04	0.99	✓		✓	✓	✓		✓	✓	✓		✓	✓	✓		✓	✓	✓		✓	✓
09/27/04	1.00	✓		x	✓	✓		x	✓	✓		x	✓	✓		x	✓				
10/04/04	1.04	✓		x	✓	✓		x	✓	✓		x	✓	✓		x	✓				
10/07/04	1.11	✓		x	✓	✓		x	✓	✓		x	✓	✓		x	✓				
10/13/04	1.15	✓		x	✓	✓		x	✓	x		x	✓	✓		x	✓				
12/06/04	1.20	✓		x	✓	✓		x	✓	✓		x	✓	✓		x	✓				
12/13/04	1.40	✓		x	✓	✓		x	✓	✓		x	✓	✓		x	✓				
12/17/04	1.46	✓		x	✓	✓		x	✓	✓		x	✓	✓		x	✓				
01/04/05	1.50	✓		x	✓	✓		x	✓	✓		x	✓	✓		x	✓				
* Wheel load in kN						¹ Measurements at 4, 6, 8, 10, and 12						² Measurements at 4, 8, and 12									
✓	Data collected	x						Suspect data, not used						No data collection scheduled							

Table 2.2: Summary of MDD and RSD Measurements (cont)

Date	Reps (x1million)	MDD4				MDD8				MDD12				RSD Centerline ¹				RSD Sides ²				
		60*	90	80	100	60	90	80	100	60	90	80	100	60	90	80	100	60	90	80	100	
01/12/05	1.58	✓		x	✓	✓		x	x	✓		x	✓	✓		x	✓					
01/19/05	1.70	✓		x	✓	✓		x	✓	✓		x	✓	✓		x	✓					
01/24/05	1.80	✓		x	✓	✓		x	✓	✓		x	✓	✓		x	✓					
02/01/05	1.90	✓		x	✓	✓		x	✓	✓		x	x	✓		x	✓					
02/07/05	2.01	✓	✓	✓	✓	✓	✓	✓	✓	✓	✓	✓	✓	✓	✓	✓	✓	✓	✓	✓	✓	✓
* Wheel load in kN						¹ Measurements at 4, 6, 8, 10, and 12						² Measurements at 4, 8, and 12										
✓	Data collected					x	Suspect data, not used										No data collection scheduled					

3. DATA SUMMARY

This chapter provides a summary of the data collected from Section 589RF, and a brief discussion of the first-level analysis. Interpretation of the data in terms of pavement performance will be discussed in a separate second-level analysis report.

3.1. Temperatures

Pavement temperatures were controlled using the temperature control chamber. Both air (inside and outside the temperature box) and pavement temperatures were monitored and recorded hourly during the entire loading period. Figure 3.1 illustrates the frequencies of recorded temperatures at each hour in the testing period from June 23, 2004 to February 08, 2005, a total of 230 days. Hourly temperatures were collected for approximately 78 percent of the test period. No temperatures were recorded during the periods of breakdown or shutdown. As seen in the figure, the hour counts from 09:00 to 14:00 hours (on a 24-hour clock) are relatively low, this being the period when measurements were taken. As a consequence, temperature interpolation/extrapolation will be necessary when interpreting the backcalculation results from the MDD and RSD measurements (second-level analysis). In assessing fatigue performance, the temperature at the bottom of the asphalt concrete and the temperature gradient are the two important controlling temperature parameters used to evaluate the stiffness of the asphalt concrete and to compute the maximum tensile strain as accurately as possible.

3.1.1 Air Temperatures in the Temperature Control Unit

Air temperatures inside the temperature control chamber ranged from 14°C to 25°C during the entire testing period. Temperatures were adjusted to maintain a pavement temperature at 50 mm depth of 20°C±4°C for the first one million repetitions and 15°C±4°C for the remainder of the test. These temperature ranges are expected to promote fatigue damage leading to reflective cracking while minimizing rutting of the asphalt concrete layer. Testing was stopped when the temperature went out of range. The temperature distributions for the various stages of the test were:

- Zero to one million repetitions: mean of 21.2°C with a standard deviation of 1.5°C (minimum 20 C, maximum 25°C).
- One million to end of test: mean of 15.6°C with a standard deviation of 2.1°C (minimum 14.0°C, maximum 19.0°C).

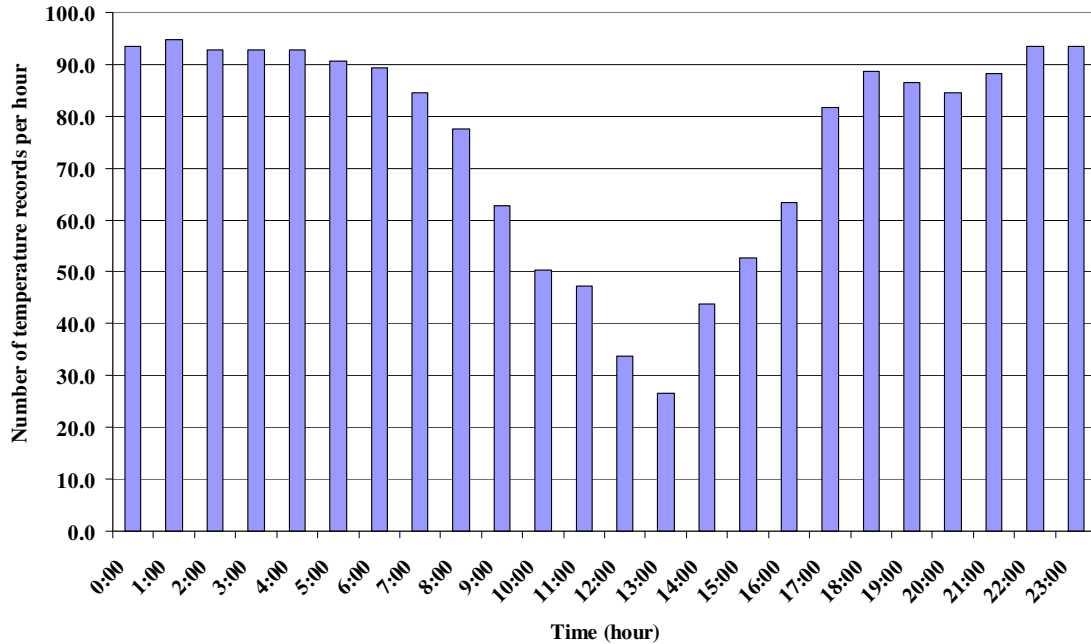


Figure 3.1: Frequencies of recorded temperatures.

The daily average temperatures recorded in the temperature control unit, calculated from the hourly temperatures recorded during HVS operation, are shown in Figure 3.2. Vertical error bars on each point on the graph show daily temperature range.

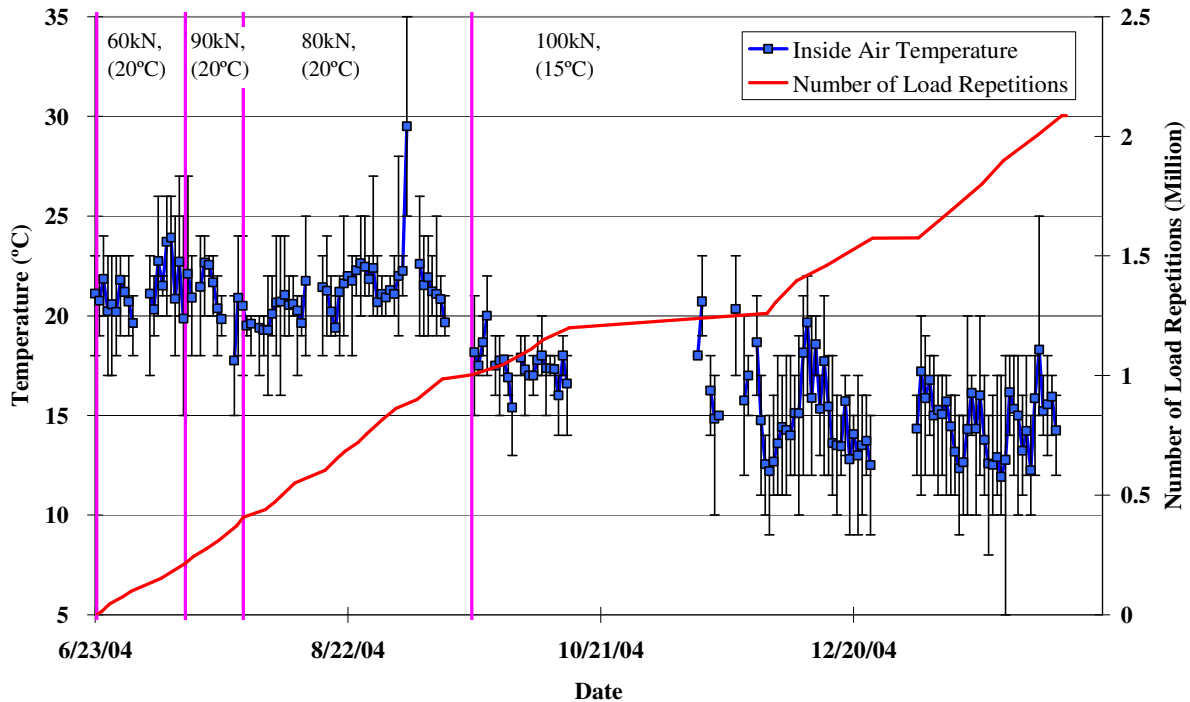


Figure 3.2: Daily average air temperatures inside the temperature control chamber.

3.1.2 Outside Air Temperatures

Outside air temperatures ranged from 7.0°C to 23.0°C with an average of 13.5 C and are summarized in Figure 3.3. Vertical error bars on each point of the graph show daily temperature range.

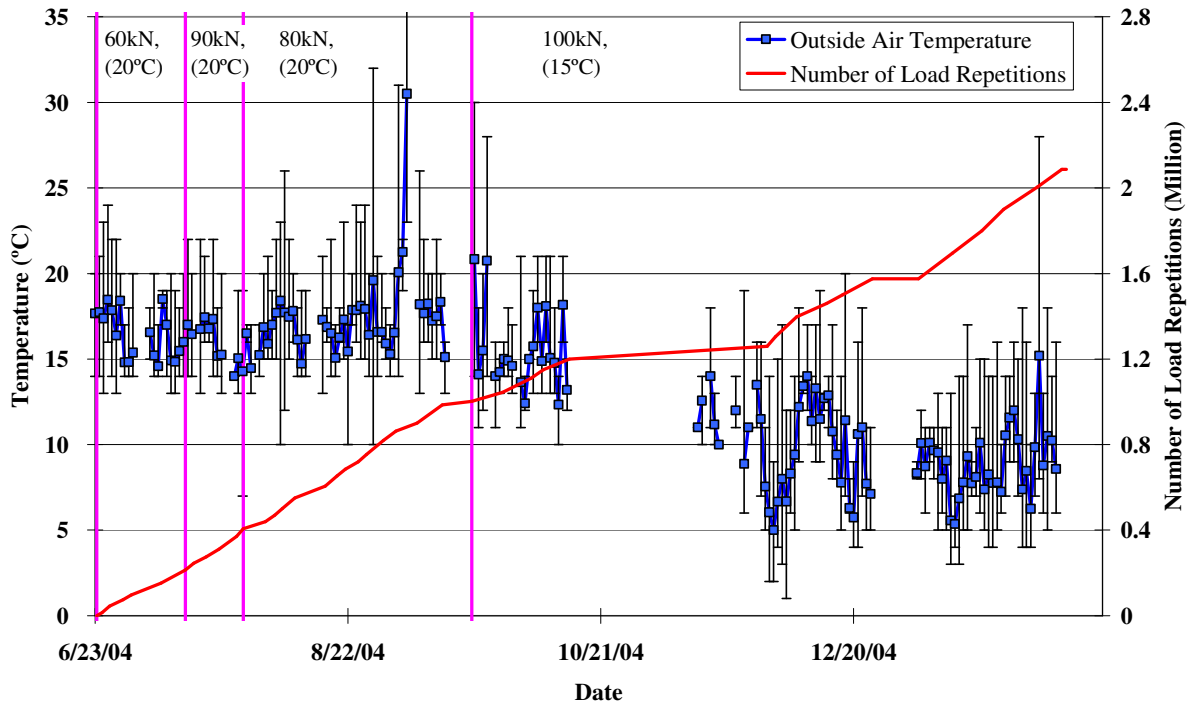


Figure 3.3: Daily average air temperatures outside the temperature control chamber.

3.1.3 Temperature in the Asphalt Concrete Layer

Daily averages of the surface and in-depth temperatures are listed in Table 3.1 and shown in Figure 3.4. Pavement temperatures increased during the early part of the test with very little difference in temperature at the various depths. After one million repetitions, pavement temperatures dropped sharply after conditioning, with temperatures at the various depths showing little variation. Pavement temperatures did not appear to be significantly influenced by outside air temperatures.

Table 3.1: Temperature Summary for Air and Pavement

Temperature	0-1,000,000		1,000,000 - 2,086,004	
	Average	Std Dev	Average	Std Dev
Outside Air	16.9	2.2	10.9	3.5
Inside Air	21.2	1.5	15.6	2.1
Pavement Surface	21.1	0.8	15.0	1.5
- 25-mm below surface	21.3	0.8	15.6	1.3
- 50-mm below surface	21.4	0.8	15.3	1.4
- 90-mm below surface	21.3	0.7	15.3	1.5
- 120-mm below surface	21.4	0.7	15.4	1.5

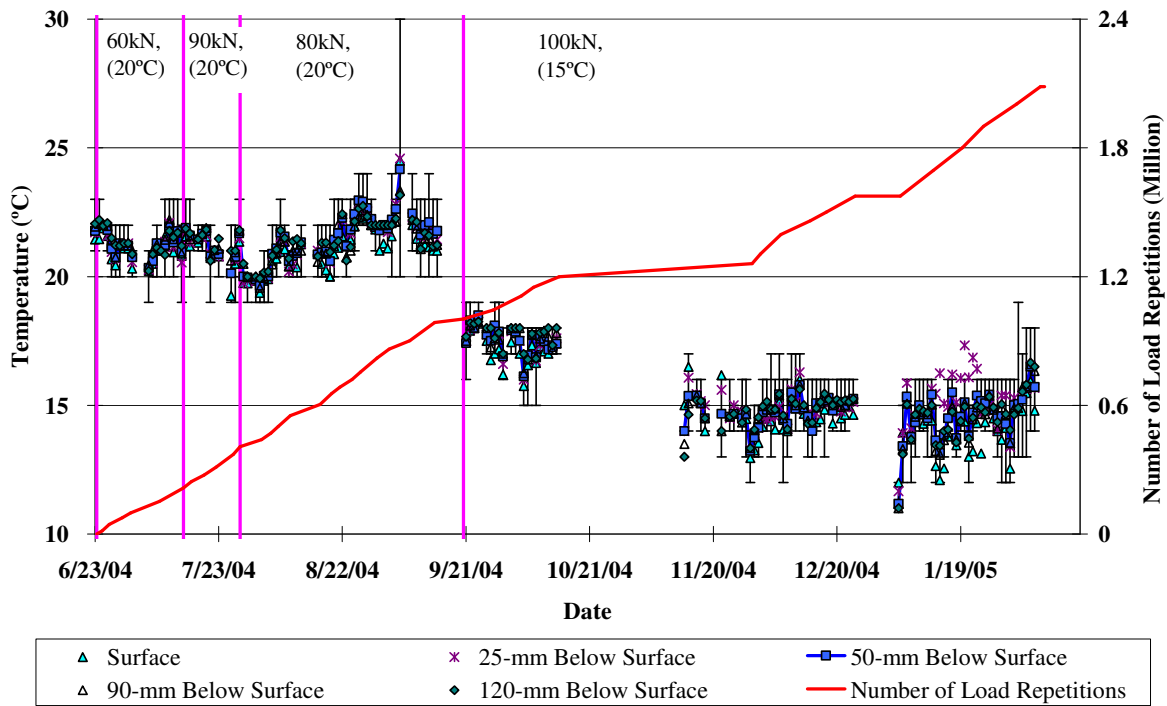


Figure 3.4: Daily average temperatures at pavement surface and various depths.

3.2. Rainfall

Figure 3.5 shows the monthly rainfall data from September 2001 to February 2003 as adapted from the Richmond Field Station HVS site and from the National Climatic Data Center (NCDC) recording station in Richmond.

3.3. Elastic Deflection

Elastic (recoverable) deflections provide an indication of the overall stiffness of the pavement structure and, therefore, a measure of the load-carrying capacity. As the stiffness of a pavement structure deteriorates, its ability to resist the deformation/deflection caused by a given load and tire pressure decreases. During HVS testing elastic deflections are measured with two instruments: the RSD to measure surface deflections and the MDD to measure in-depth deflections. MDD modules could not be installed at the surface (0 mm) due to the limited thickness of the overlay and thus it is not possible to directly compare surface deflections between the two instruments. In addition to RSD and MDD measurements, FWD measurements were taken before and after HVS trafficking to evaluate the initial and final conditions of the pavement.

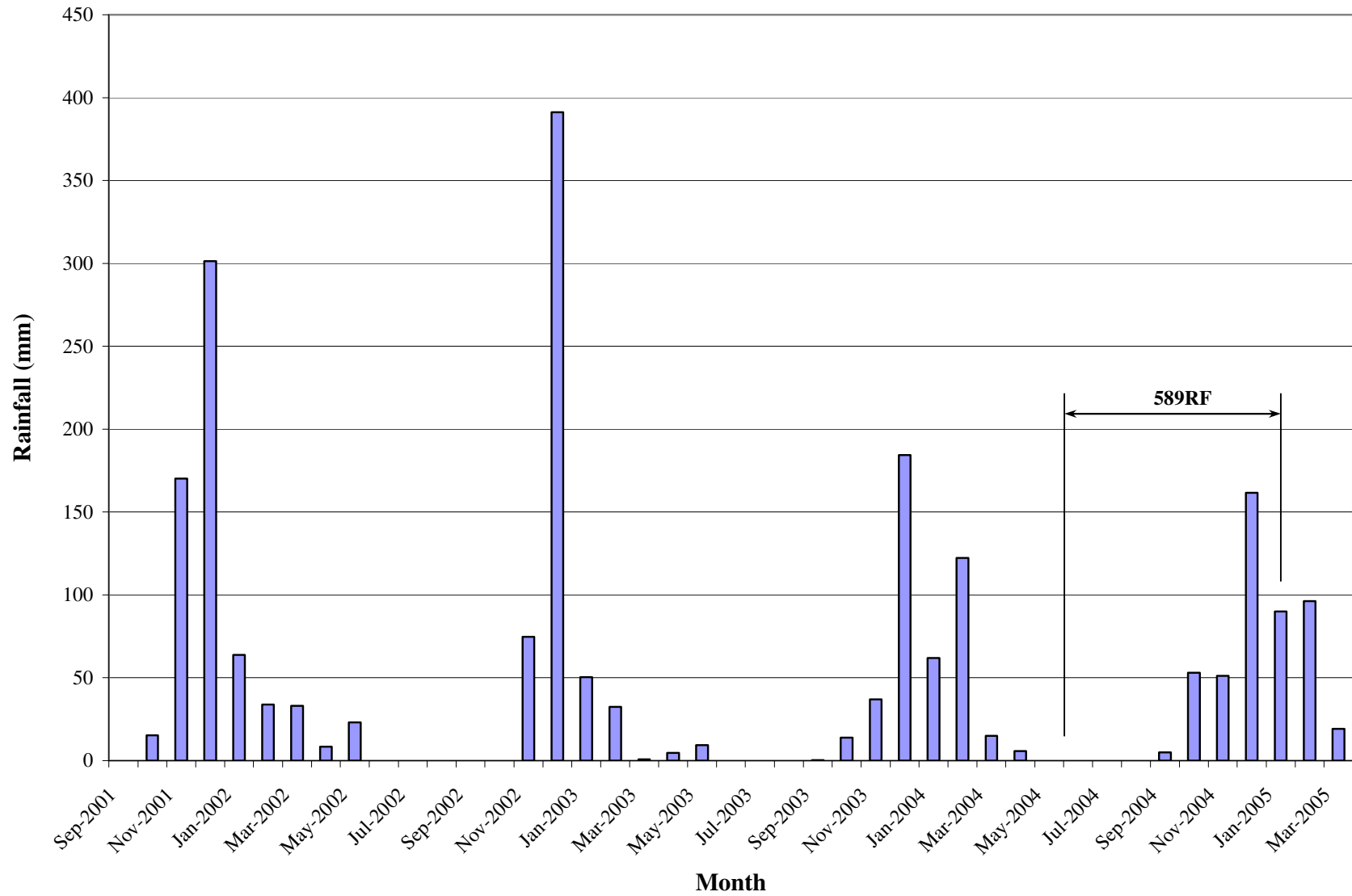


Figure 3.5: Monthly rainfall for Richmond Field Station.

3.3.1 Surface Elastic Deflection Using RSD

In this section of the report, surface deflections as measured by the RSD under a load of 60 kN are summarized (note that the HVS trafficking load does not remain the same during the course of the experiment).

Table 3.2 compares the average 60 kN RSD deflections for centerline locations 4, 6, 8, 10, and 12 before and on completion of testing. The relatively high standard deviation for the average deflection after trafficking is attributed to variability in the cracking of the underlying DGAC layer, which is discussed below.

Table 3.2: Average 60 kN RSD Centerline Deflections Before and After Testing

Position	Parameter	Deflection (microns)		
		Before Trafficking	After Trafficking	Ratio of Final/Initial
All	Average	562	1,375	2.45
	Std. Deviation	43	253	-
4CL	Average	510	1,142	2.24
6CL	Average	556	1,185	2.13
8CL	Average	535	1,289	2.41
10CL	Average	614	1,516	2.47
12CL	Average	598	1,747	2.92

At the start of the test, initial deflections were all within 0.1 mm of each other, with higher deflections (i.e., weaker pavement) recorded at positions 10CL and 12CL, overlying that part of the DGAC with the highest density of cracking. During the course of the test, substantial damage occurred on the overlay over the entire section under HVS trafficking, with higher values at the end overlying the severely cracked DGAC. This is confirmed by the ratio of final-to-initial deflections for all RSD locations, which show that surface deflections increase by between two and three times along the length of the test section, indicating significant damage in the pavement structure in terms of loss of stiffness. Although the ratio of final-to-initial deflections is fairly consistent across the section, when the results are considered in conjunction with Figure 2.3, lower deflections (4CL and 6CL) were recorded at the end of the section that had the least amount of cracking in the underlying pavement (stiffer pavement), while those with the highest deflections (8CL, 10CL, and 12CL) are over the more severely cracked area (weaker pavement).

Deflections and damage rates both increased with increase in load. Figures 3.6 to 3.10 compare the deflection bowls at the same locations at test start, at load change intervals, and at test completion. The same scale is used on all figures, and the increasing deflection over time and with load is clearly evident. The higher deflections at points 8CL, 10CL, and 12CL over the cracked underlying DGAC can be observed.

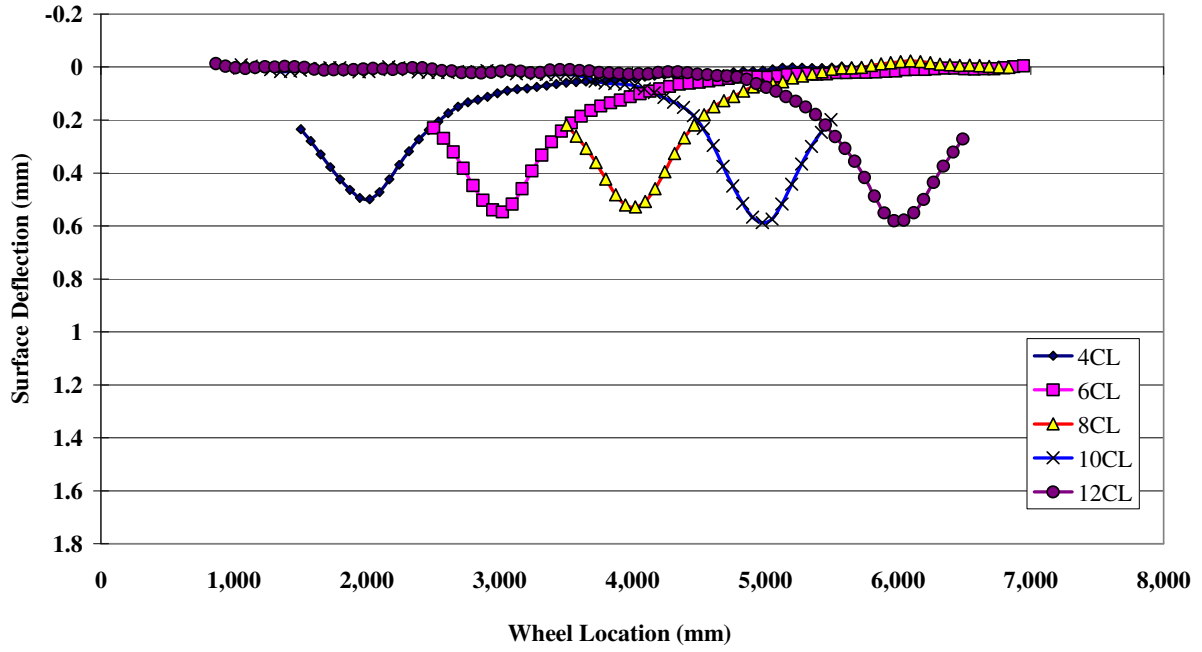


Figure 3.6: RSD deflections at CL locations with 60 kN test load at test start.

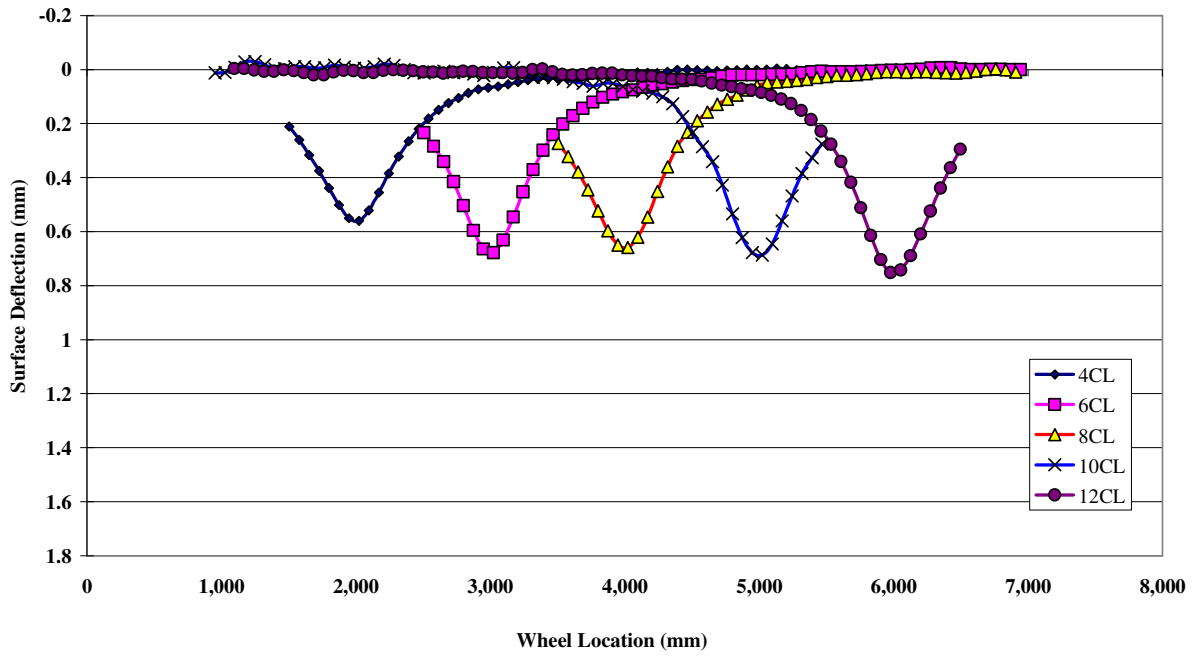


Figure 3.7: RSD deflections at CL locations with 60 kN test load after 215,000 repetitions.

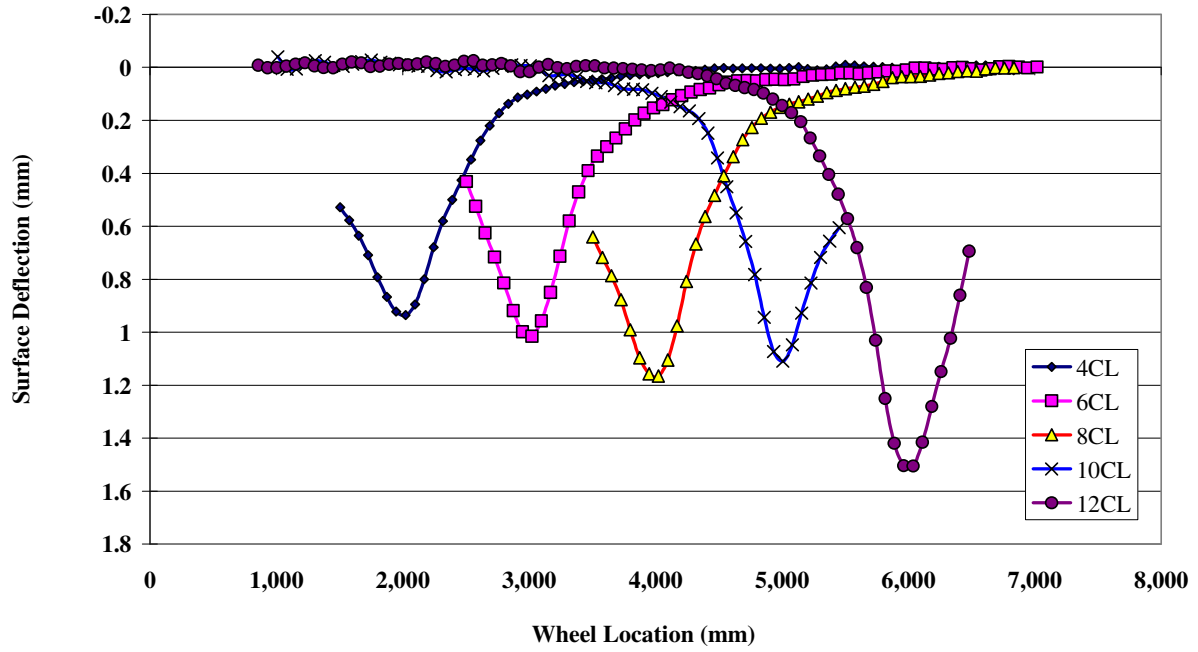


Figure 3.8: RSD deflections at CL locations with 60 kN test load after 407,197 repetitions.

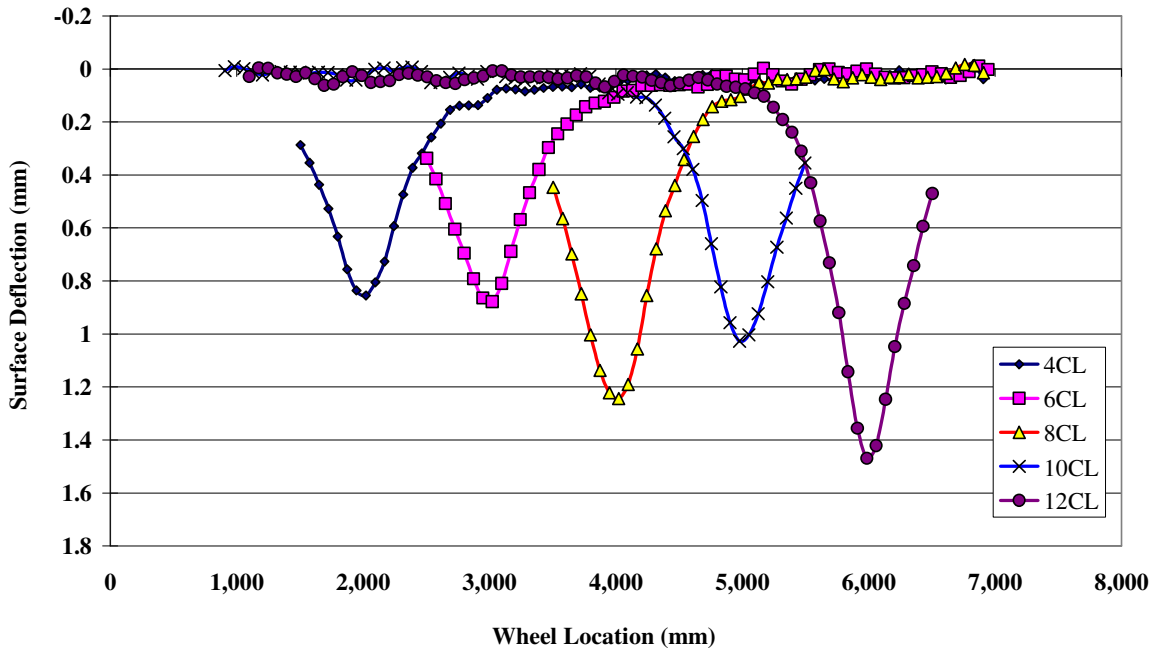


Figure 3.9: RSD deflections at CL locations with 60 kN test load after 1,002,000 repetitions.

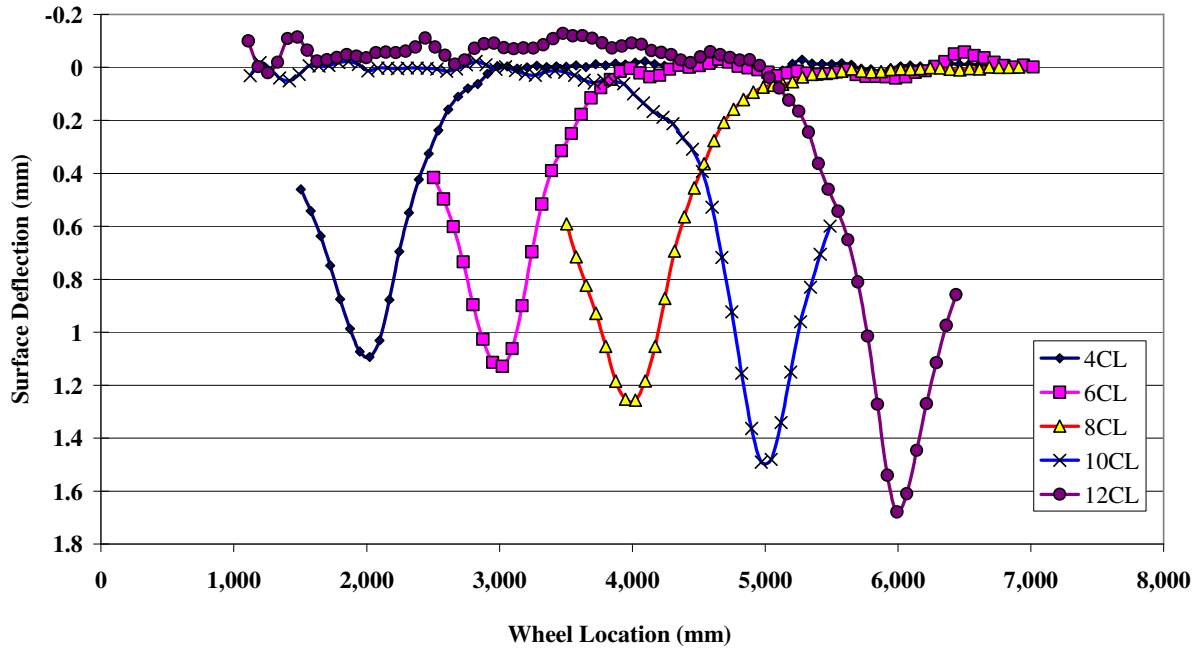


Figure 3.10: RSD deflections at CL locations with 60 kN test load at test completion.

The average 60 kN RSD deflections at centerline and side locations (200 mm from centerline within the trafficked area) are illustrated in Figure 3.11. These deflections are mostly all within 0.2 mm of each other, although as expected the side deflections are less than those of the centerline. These results indicate that damage was somewhat greater in the vicinity of the centerline compared to the area away from the centerline where fewer repetitions are applied by the programmed wander of the HVS trafficking pattern.

Figure 3.12 shows the average 60 kN deflection at centerline as well as the averages for measurements taken at the end of the section with more severely cracked DGAC underneath (8CL, 10CL and 12CL) and the end with less severe cracking (4CL and 6CL). The difference in deflections is evident between the two ends. In Figures 3.11 and 3.12, some sensitivity of RSD deflection to temperature is evident, for example at approximately 550,000, 863,000, at the load change at 1,002,000, and at 1,200,000 repetitions. The influence of temperature on deflection will be discussed in the second-level analysis report. The sensitivity of the RSD to a load reduction is evident in the early phase of 80 kN loading.

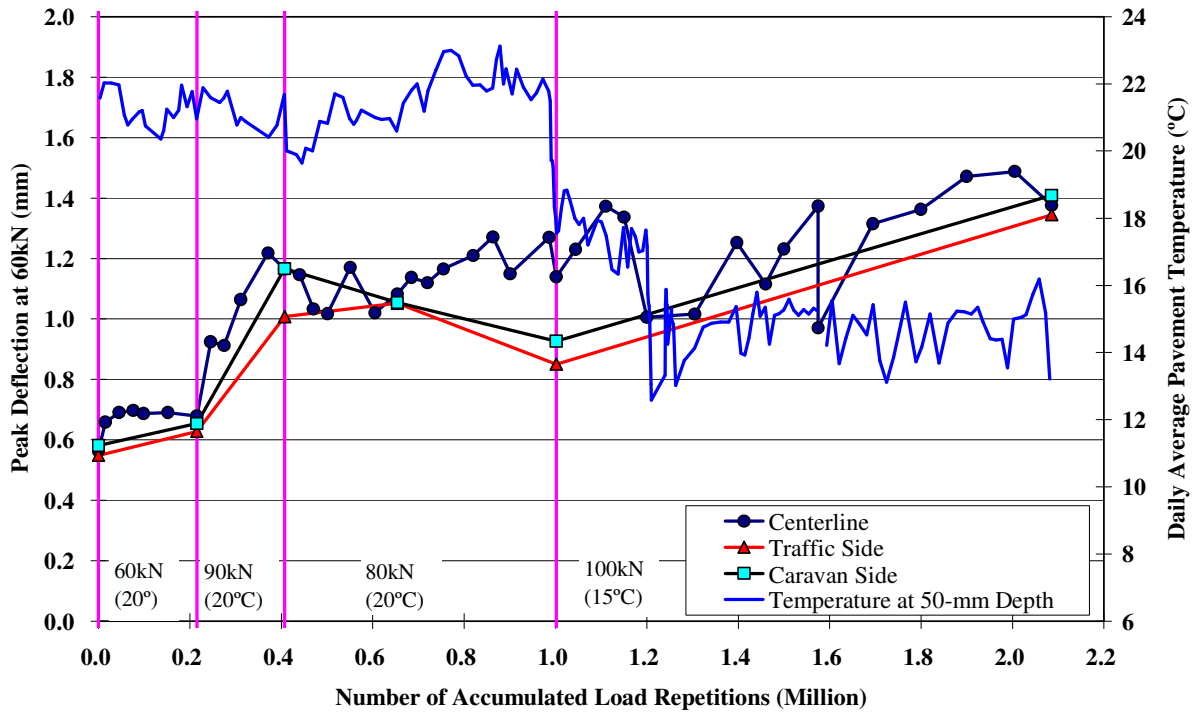


Figure 3.11: Average RSD surface deflections with 60 kN test load (centerline and sides).

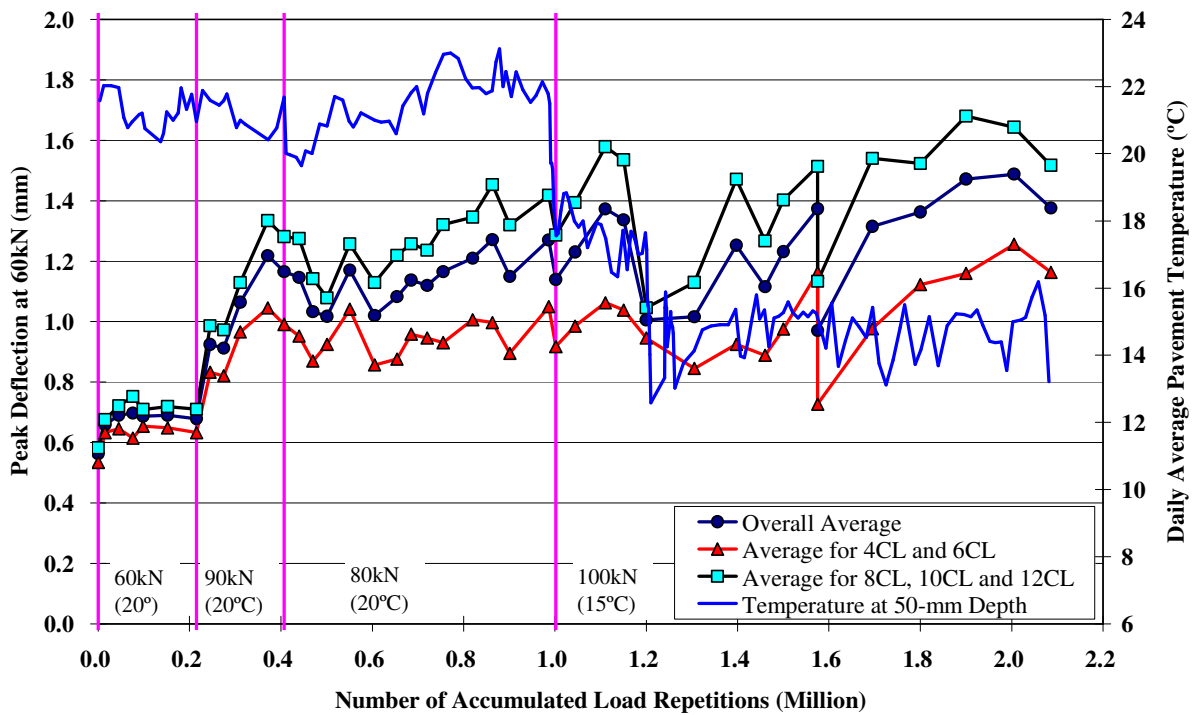


Figure 3.12: Average RSD surface deflections with 60 kN test load (centerline and subsection).

3.3.2 Surface Elastic Deflection Using FWD

FWD testing was conducted on the section before and after HVS trafficking to monitor the changes in layer moduli. Table 3.3 summarizes the date, location, temperatures, and average deflections for the section. Temperatures listed are average temperatures. Recordings from two sensors (1 and 6) and two locations (section centerline and side of section) are shown. Sensor 1 (the sensor directly under the falling weight) provides an indication of the deflection of the composite pavement. Sensor 6 provides an indication of the deflection in the subgrade. Centerline readings show deflection on the trafficked area, while readings from the side of the section are used to compare trafficked and untrafficked areas. Figures 3.13 through 3.17 show the FWD deflection measurements recorded on the section. Note that scales differ between plots. Backcalculation of these results will be discussed in the second-level analysis report.

Table 3.3: Summary of FWD Measurements

Date	Location	Temperatures (°C)		FWD Deflection at 40 kN (microns) ¹			
		Air	Surface	Sensor 1		Sensor 6	
				Average	Std. Dev.	Average	Std. Dev.
After completion of Section 571RF							
10/10/02	Centerline	N/A	20.1	322	78	49	2
Before start of Section 589RF							
2/18/05	Centerline	14.3	18.4	104	10	36	3
6/21/05	Centerline	N/A	27.2	201	29	50	1
After completion of Section 589RF							
02/24/05	Centerline	10.9	13.4	359	152	58	19
02/18/05	Centerline	15.6	20.0	401	153	55	6
02/23/05	Side ²	10.7	11.4	211	34	72	8
02/18/05	Side	15.8	17.1	230	56	66	8

¹ Deflections based measurements between Stations 3 and 13 inclusive

² Side location is 1.0 m from the test section, representing untrafficked area

Figure 3.13 shows the effect of damage on the pavement over the course of the experiment. Deflection measured on Section 571RF prior to placing the overlay was relatively high, especially in the area of more severe cracking. Placement of the overlay considerably reduced the deflection. However, considerable damage was again caused by the HVS trafficking, with higher after-test damage recorded on parts of the section (Stations 10 through 14) than were recorded after testing ended on Section 571RF. The overlay does not appear to have provided any significant structural improvement over the area with less severe cracking (Stations 0 through 4). The figure also shows that deflections were generally influenced by temperature, with lower deflections measured in the morning (lower temperature) compared to those measured in the afternoon (higher temperature) at the end of the test.

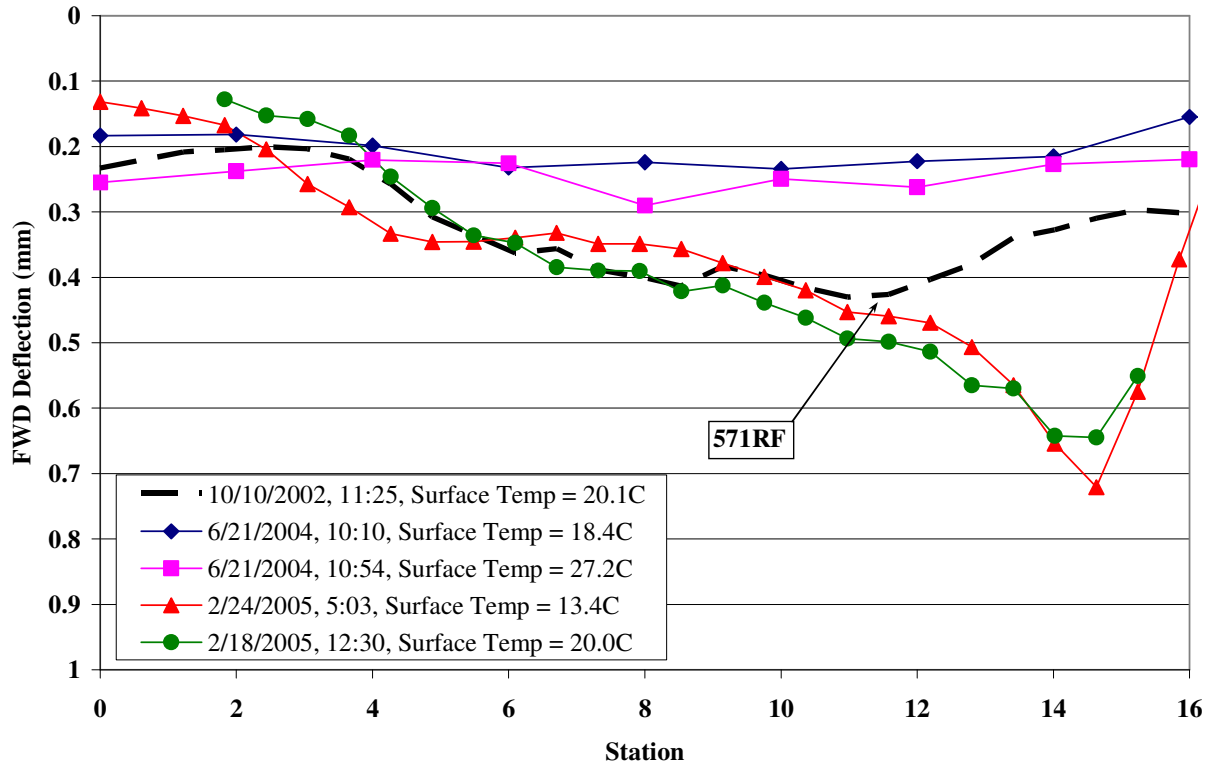


Figure 3.13: Composite pavement stiffness (FWD Sensor 1) on section centerline.

Figure 3.14 shows deflections in the subgrade before and after the test. These measurements indicate that there was no significant change (0.02 mm) during the course of the experiment, although some damage can be noted at the end of the section with more severe cracking (Stations 10 through 14) after trafficking had been completed. The overlay did not provide any significant structural improvement to the overall pavement structure in terms of protection of the subgrade. Some temperature sensitivity was noted in the afternoon measurements prior to trafficking, when the surface temperatures were almost 10°C warmer than those recorded that morning.

Figures 3.15 and 3.16 show FWD deflections taken along the side of the HVS test section but outside the trafficked area, (i.e., the area tested did not have traffic damage). The figures can be used to understand the influence of environmental conditions on the performance of the section. Figure 3.15 shows some damage associated with HVS testing between Stations 10 and 14, which is attributed to the severe rutting at that end of the section. This is discussed in more detail in Section 3.4. However, the subgrade showed almost no change over the course of the experiment. The off-section deflections did not appear to be significantly influenced by temperature.

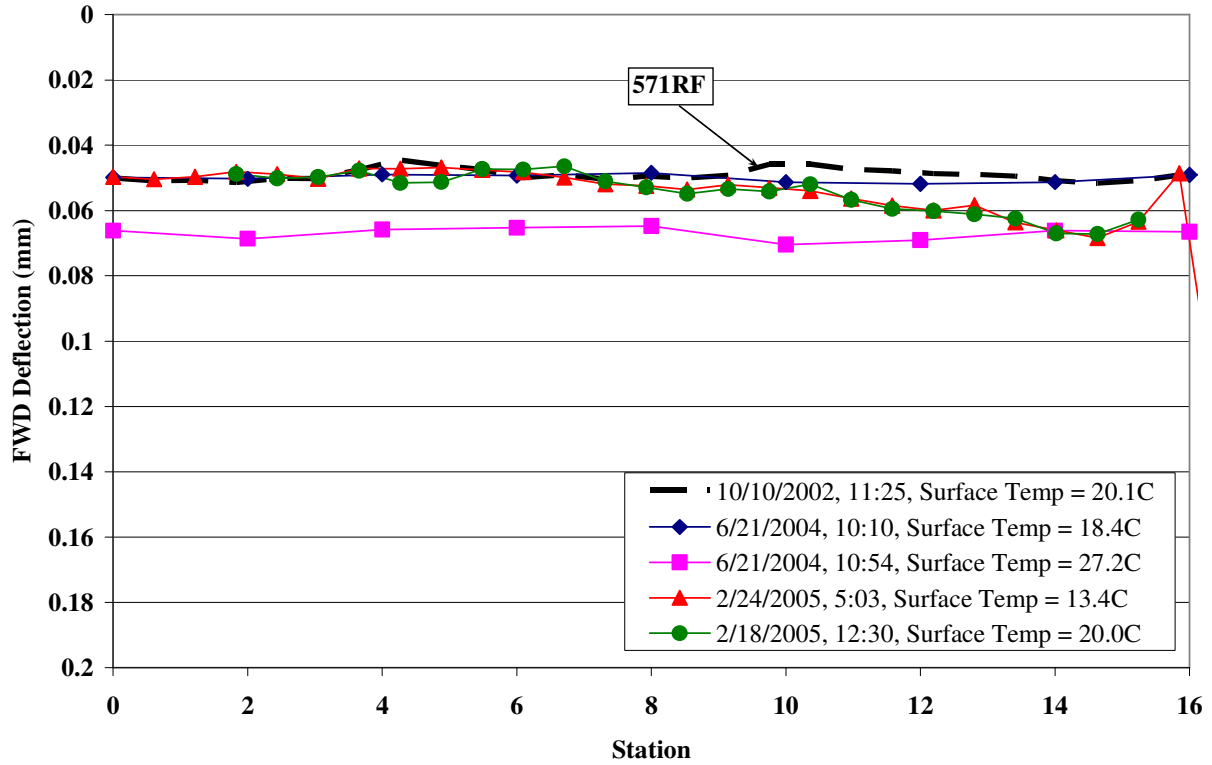


Figure 3.14: Subgrade pavement stiffness (FWD Sensor 6) on section centerline.

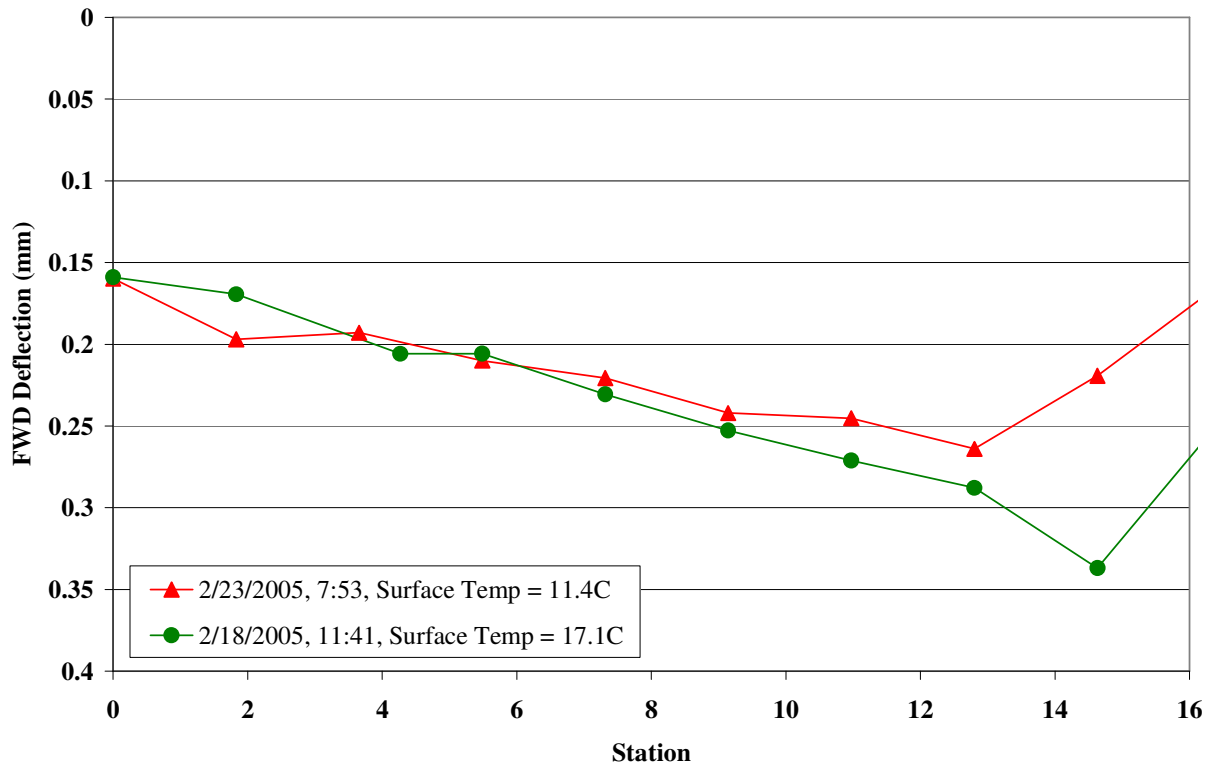


Figure 3.15: Composite pavement stiffness (FWD Sensor 1) outside trafficked area.

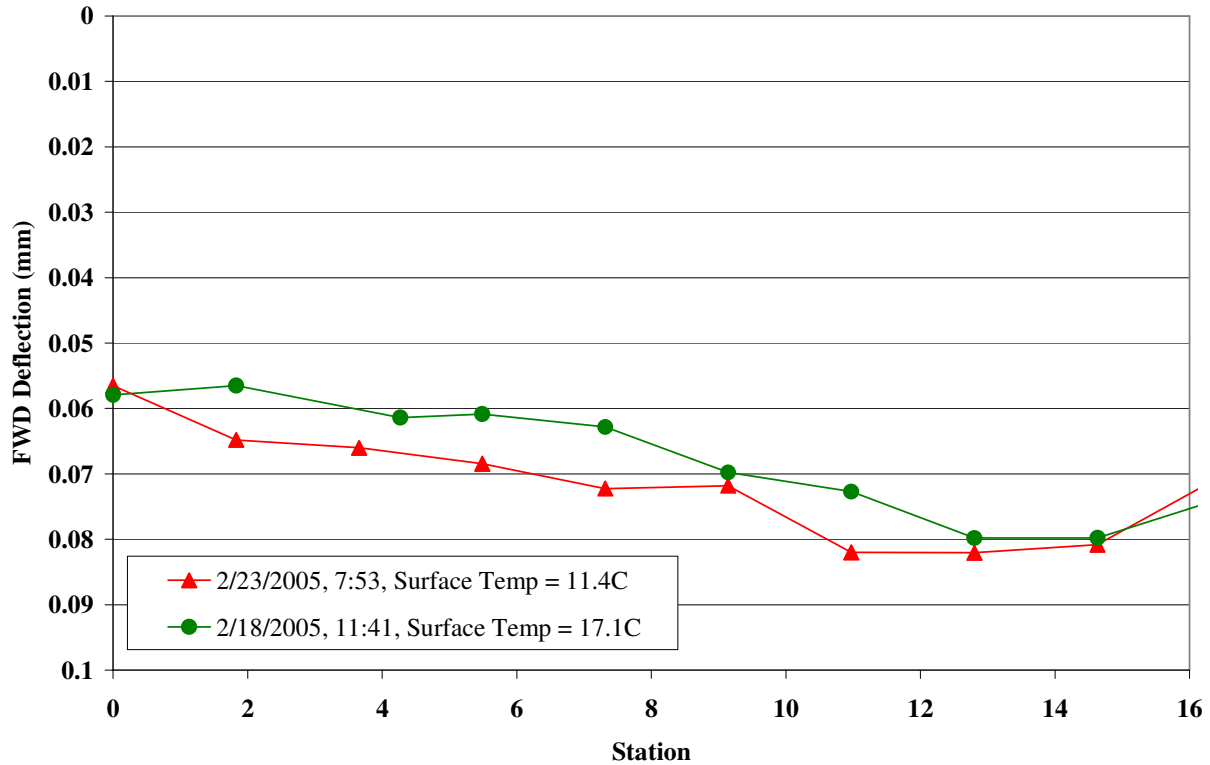


Figure 3.16: Subgrade pavement stiffness (FWD Sensor 6) outside trafficked area.

3.3.3 In-depth Elastic Deflection

The schedule of MDD measurements with various test loads is listed in Table 2.2. Data acquisition and MDD linear variable displacement transducer (LVDT) problems resulted in some questionable data being collected at various times through the experiment and specifically at the 90 kN, 80 kN, and 100 kN test loads. In line with other reports in this study, the following discussion will focus on results obtained with the 60 kN load only.

Table 3.4 and Figures 3.17 through 3.19 summarize the in-depth elastic deflections measured at various depths with MDDs 4, 8 and 12 respectively. The figures include RSD measurements taken on the surface at the same locations as the MDDs. Note that scales differ for each instrument.

Table 3.4: Summary of 60 kN In-depth Elastic Deflections

Depth (mm)	Layer	Elastic Deflection (microns)		
		Before Trafficking	After Trafficking	Ratio of Final/Initial
MDD4				
0	Surface (from RSD)	510	1,140	2.24
132	Bottom of cracked DGAC	510	997	1.95
337	Middle of aggregate base	462	782	1.69
542	Bottom of aggregate base	374	628	1.68
847	300 mm below top of subgrade	205	320	1.56
MDD8				
0	Surface (from RSD)	535	1,553	2.90
132	Bottom of cracked DGAC	N/A	1,289	-
337	Middle of aggregate base	380	1,101	2.90
542	Bottom of aggregate base	281	847	3.01
847	300 mm below top of subgrade	269	389	1.45
MDD12				
0	Surface (from RSD)	688	1,747	2.54
132	Bottom of cracked DGAC	N/A	N/A	-
337	Middle of aggregate base	N/A	N/A	-
542	Bottom of aggregate base	593	N/A	-
847	300 mm below top of subgrade	498	N/A	-

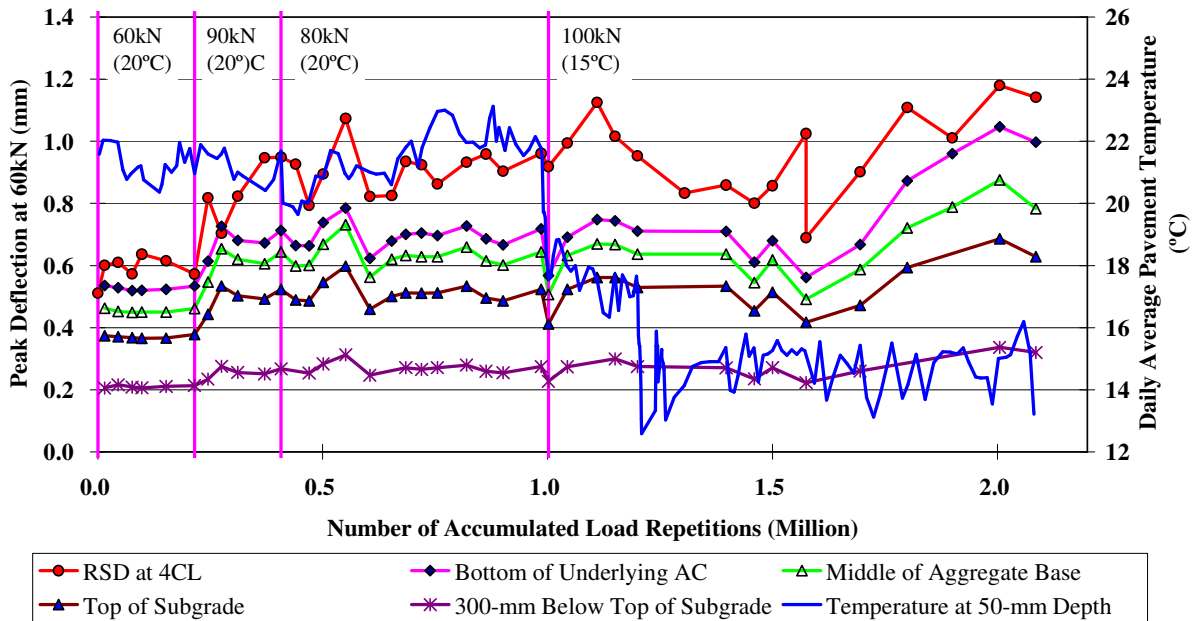


Figure 3.17: Elastic deflections at MDD4 with 60 kN test load.

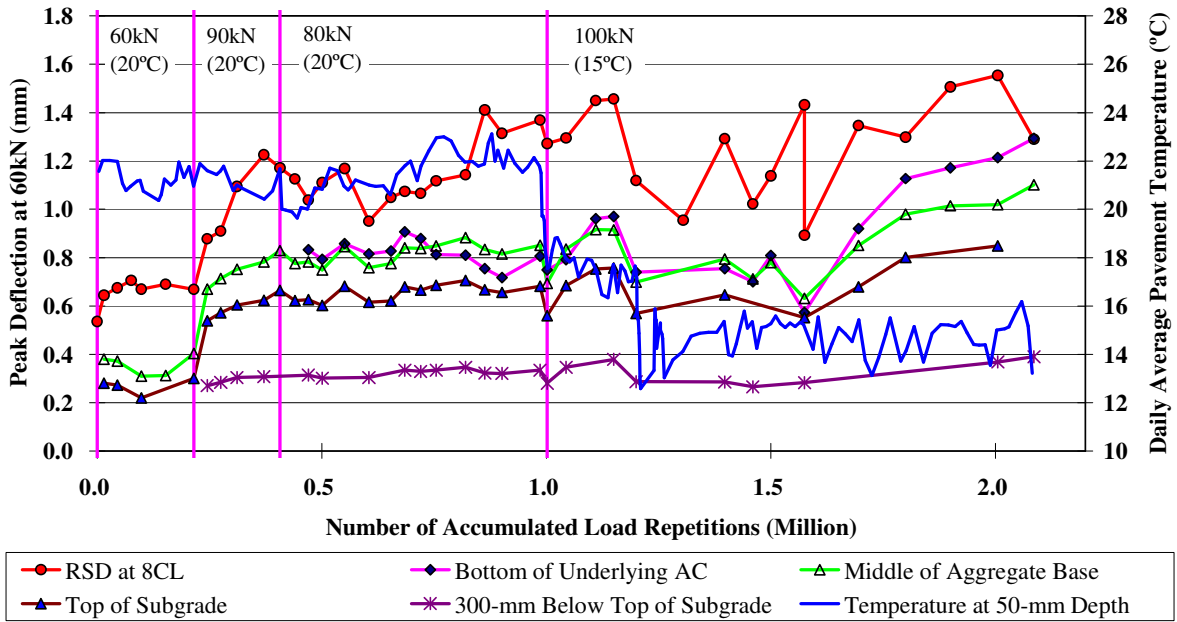


Figure 3.18: Elastic deflections at MDD8 with 60 kN test load.

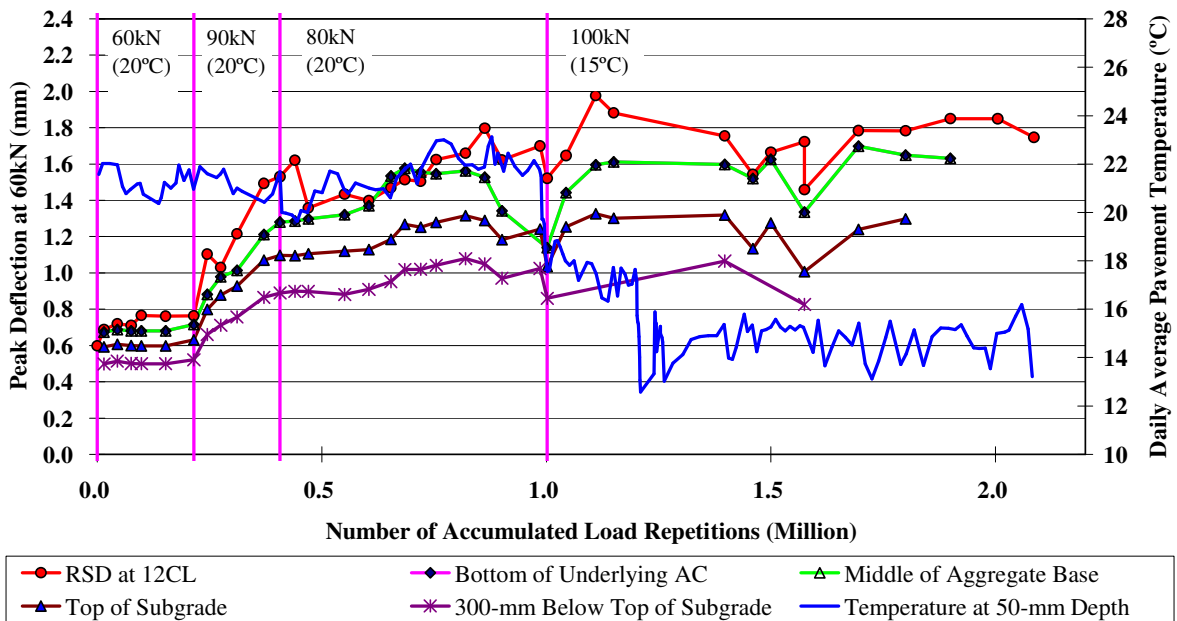


Figure 3.19: Elastic deflections at MDD12 with 60 kN test load.

The following observations were made from the data collected:

- At MDD4 (overlay on less severe cracking) very little damage was recorded during the 60 kN phase, apart from an initial increase measured on the surface, which is typical for new experiments. After the 90 kN load change, the damage rate climbs sharply at all levels during the first approximately 70,000 repetitions at the new load before steadying for the remainder of the phase. The damage rate initially drops at all levels with load decrease at the 80 kN load change.

Thereafter it increases slowly with increasing repetitions. Some temperature sensitivity can be noted during this phase, for example, at 550,000 and 680,000 repetitions. At the 100 kN load change (1,002,000 repetitions), the damage rate increases at the surface, but appears to decrease in the layers as a result of the change in temperature from 20°C to 15°C. Thereafter the damage rate increases again at all levels during a period of approximately 115,000 repetitions before steadying for about 300,000 repetitions. After approximately 1.5 million repetitions, the damage rate starts to increase again and continues to do so until the end of the experiment. Similar rates of damage can be noted in the asphalt concrete layers and in the aggregate base, with a lower rate recorded in the subgrade.

- At MDD8 (overlay on area of more severe cracking), similar trends to that observed at MDD4 are evident, although damage rates are higher, probably as a result of the more severe cracking in the DGAC layer. Only marginal damage is recorded during the 60 kN load phase. A sharp increase is evident after the 90 kN load change, with damage continuing to increase at all levels throughout this loading phase. As expected, a slight decrease in the damage rate occurs after the 80 kN load change. The damage rate increases marginally through the 80 kN load phase and then drops with the decrease in temperature at the 100 kN load change. Thereafter, the rate increases, levels off, then increases rapidly until the end of the test in similar way to that discussed for MDD4. The damage rate in the subgrade is significantly less than that recorded in the asphalt concrete and aggregate base layers.
- At MDD12 (overlay on area of severe cracking), similar trends to MDD4 and MDD8 are again noted, but damage rates are higher than at the other instruments. Marginal damage is again recorded during the 60 kN load phase, with a sharp increase at all levels after the 90 kN load change. The damage rate continues to increase through the 90 kN and 80 kN load phases, with some reduction in the early part of the 80 kN loading cycle. Although there was a reduction in the damage rate with temperature decrease at the 100 kN load change, the rate increased sharply again with the increased traffic load. Questionable data was recorded after approximately 1.5 million repetitions. This may be attributed to the deformation at this end of the section (i.e., the LVDTs went out of range), which is discussed in the next section.
- The effect of trafficking load on elastic deformation decreases with increasing depth, as expected.
- Ratios of final-to-initial MDD deflections show that deflections varied depending on the severity of cracking in the underlying DGAC layer. At MDD4, ratios decreased with increasing depth (2.24 at the surface to 1.56 in the subgrade). At MDD8, deflections in the asphalt concrete and aggregate base layers were approximately three times higher at the end of the test compared to the beginning, indicating considerable damage under HVS trafficking. The final-to-initial ratio in the subgrade was 1.45, similar to that recorded at MDD4. No final-to-initial ratios are available for

MDD12. However, similar trends to that recorded for MDD8 are likely, given the extent of cracking in the DGAC layer.

3.4. Permanent Deformation

Permanent deformation at the pavement surface (rutting) was monitored with the Laser Profilometer and at various depths within the pavement with two Multi-depth Deflectometers (MDDs). These measurements are discussed below.

3.4.1 Permanent Surface Deformation (Rutting)

Deformation and rutting on HVS tests are usually analyzed using two definitions, namely maximum rut depth and average deformation (4), as illustrated in Figure 3.20. The Laser Profilometer is used to measure these distresses and provides sufficient information to evaluate the evolution of permanent surface deformation of the entire test section at various loading stages.

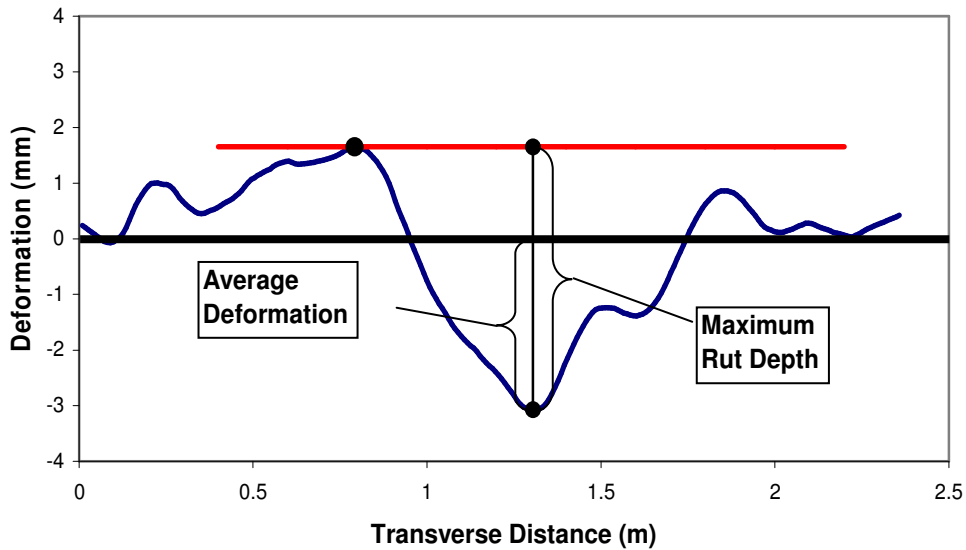


Figure 3.20: Illustration of maximum rut depth and average deformation of a leveled profile.

Figure 3.21 shows the average transverse cross section measured with the Profilometer at various stages of the test. This plot clearly shows the increase in rutting and deformation over the duration of the test.

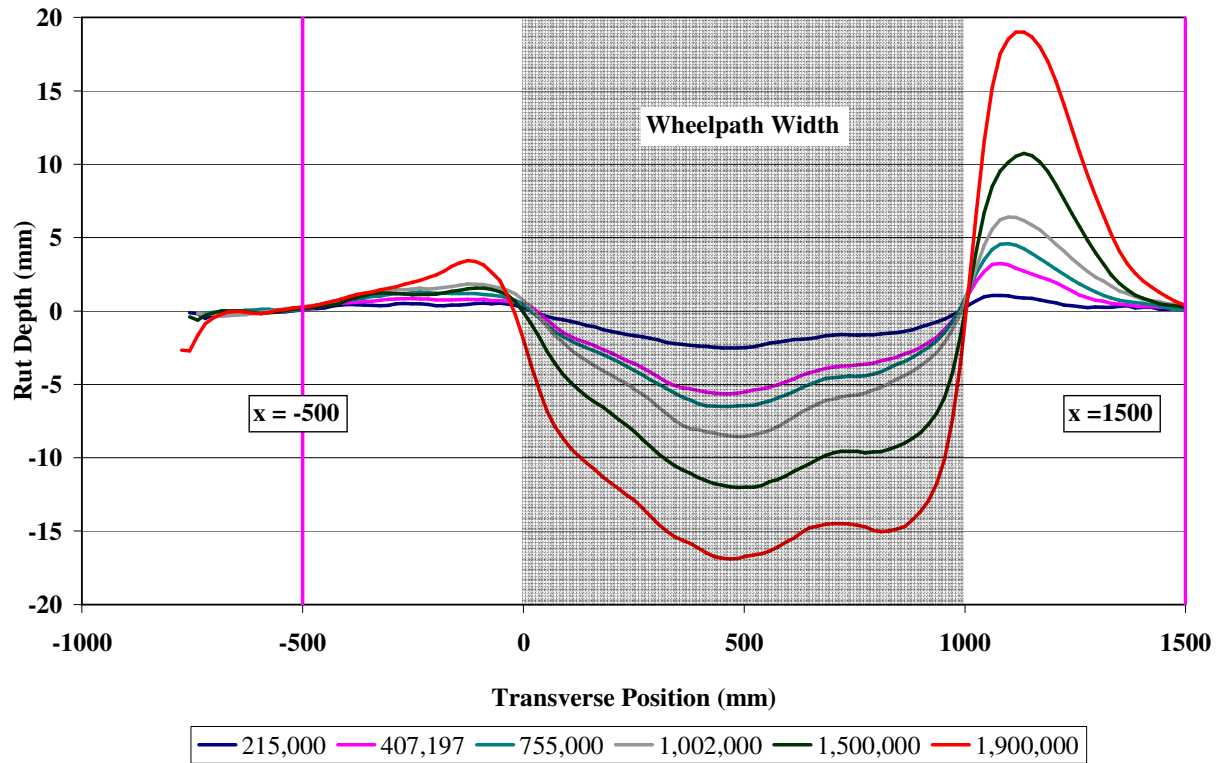


Figure 3.21: Laser profilometer cross section at various stages of trafficking.

During HVS testing, rutting usually occurs at a high rate initially and then typically diminishes as trafficking progresses until reaching a steady state. If the load level is subsequently increased, the pavement will undergo another phase of rapid rutting development until a steady phase for that new load level is reached. This initial phase is referred to as the “embedment” phase. Figures 3.22 and 3.23 show the development of permanent deformation (average deformation and maximum rut, respectively) with load repetitions as determined by the Laser Profilometer for the test section. Note that the scales on the charts are different. Embedment phases are apparent at the beginning of the experiment and at the 90 kN load change. Error bars on the average reading indicate variation along the length of the section and show a significant difference (100 mm in maximum rut) between one end of the section and the other at the end of the test. The figures also show average deformation and average maximum rut for Stations 3 to 7 and 8 to 13. Stations 3 to 7 are over the end of the section where the underlying DGAC was marginally cracked, while stations 8 to 13 are over the end with more severe cracking. The figures show that deformation and rut are considerably higher over the significantly cracked section. Deformation also continues to increase after the 100 kN load change, despite decreasing the pavement temperature to 15°C.

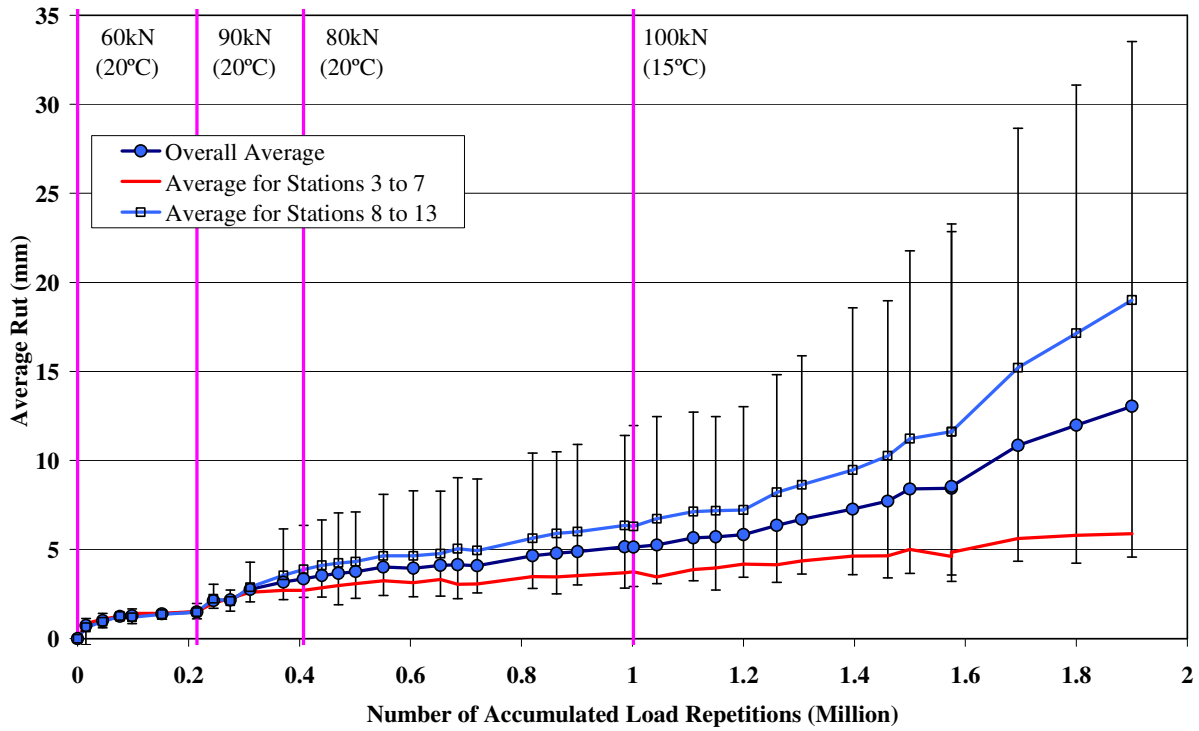


Figure 3.22: Average deformation determined from Laser Profilometer data.

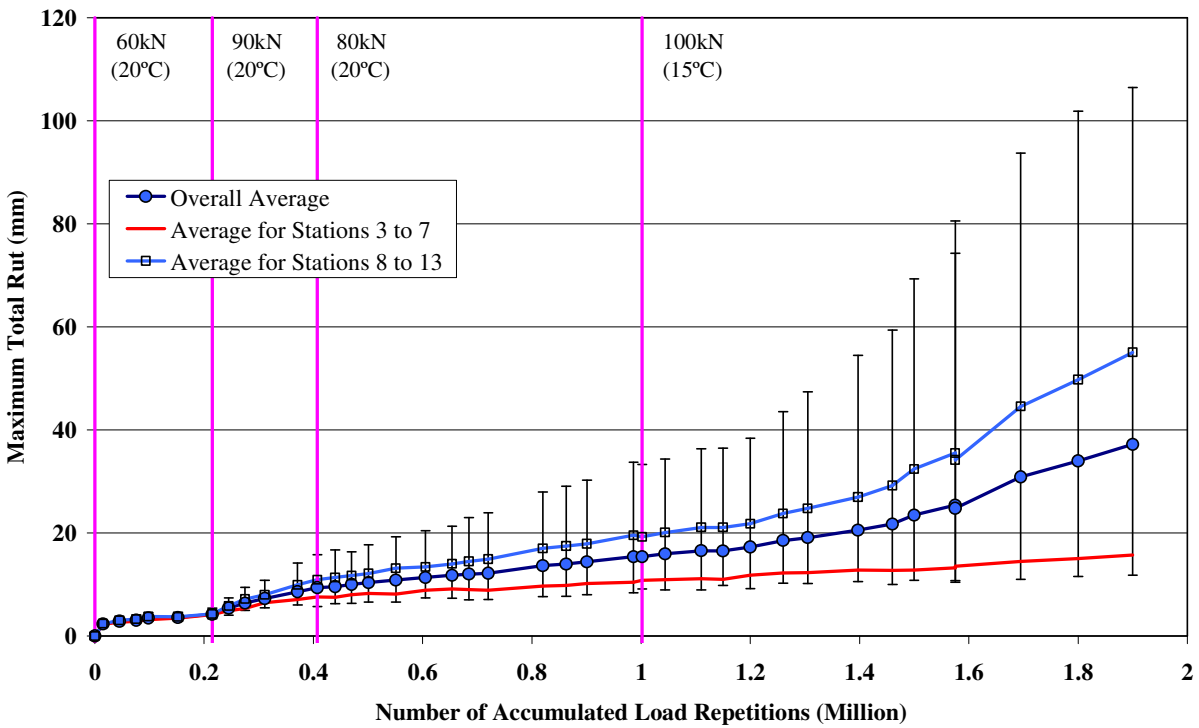


Figure 3.23: Average maximum rut determined from Laser Profilometer data.

Figure 3.24 shows a contour plot of the pavement surface at the 90 kN load change (215,000 repetitions), when a noticeable rut had started to appear at one end of the section. Figures 3.25 through 3.28 show

contour plots of the rutting progression at the 80 kN and 100 kN load changes, at 1.5 million repetitions and at the end of the test. The increase in rutting throughout the test, and especially after the 100 kN load change, is clearly evident in the figures, despite maintaining the pavement at relatively low temperatures.

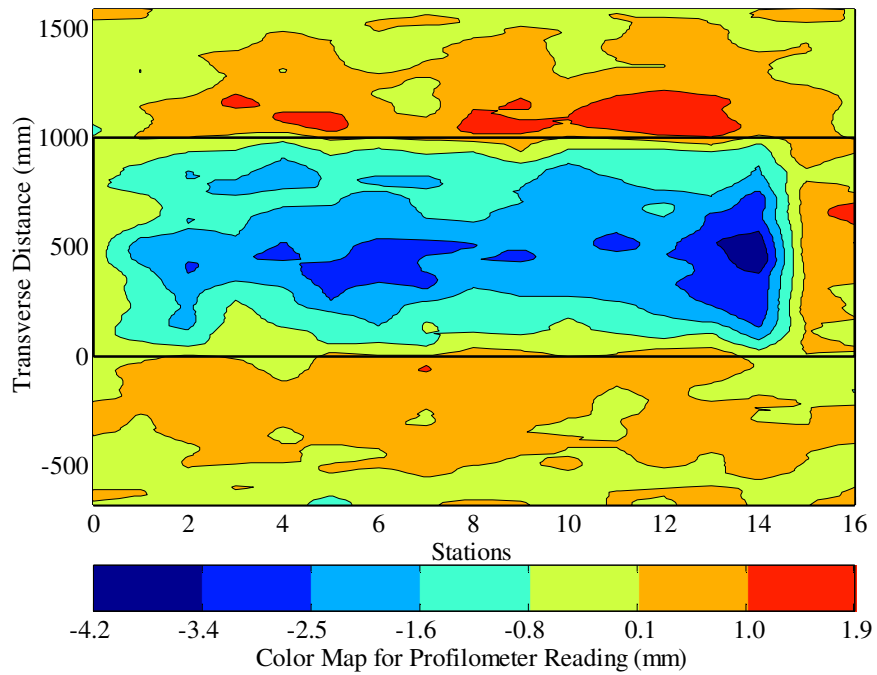


Figure 3.24: Contour plot of permanent deformation after 215,000 repetitions.

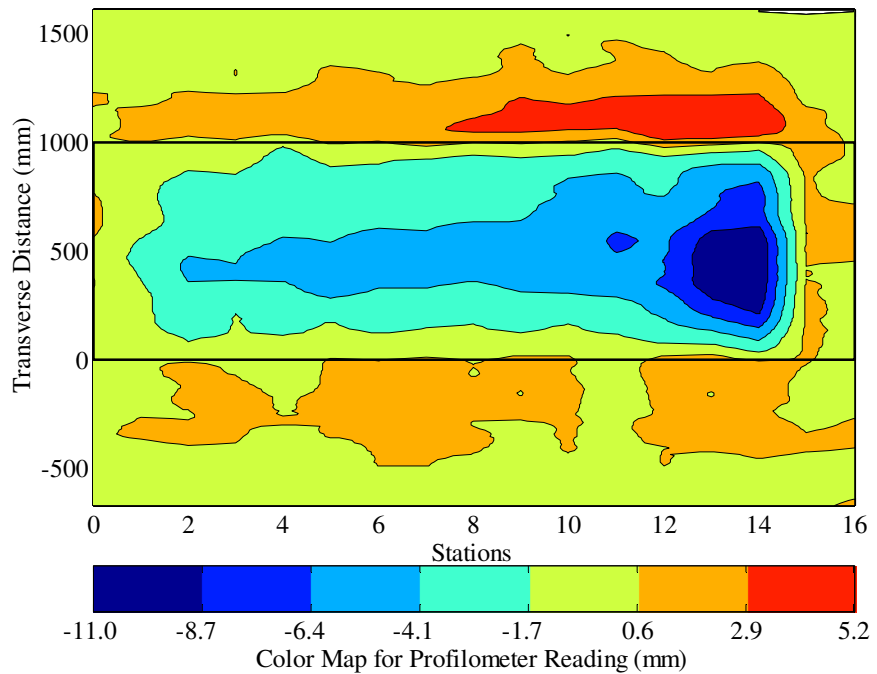


Figure 3.25: Contour plot of permanent deformation after 407,000 repetitions.

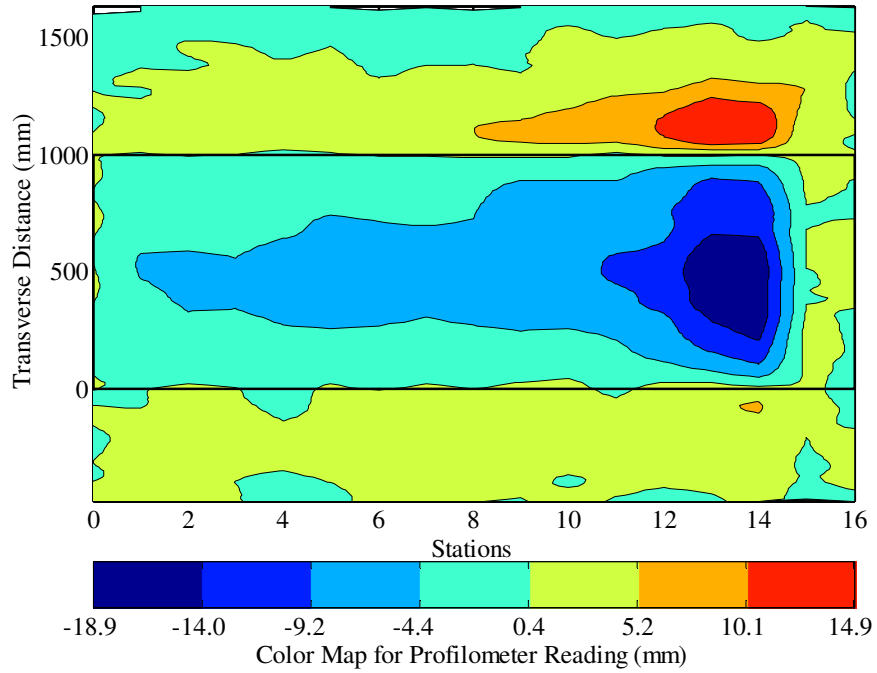


Figure 3.26: Contour plot of permanent deformation after 1,002,000 repetitions.

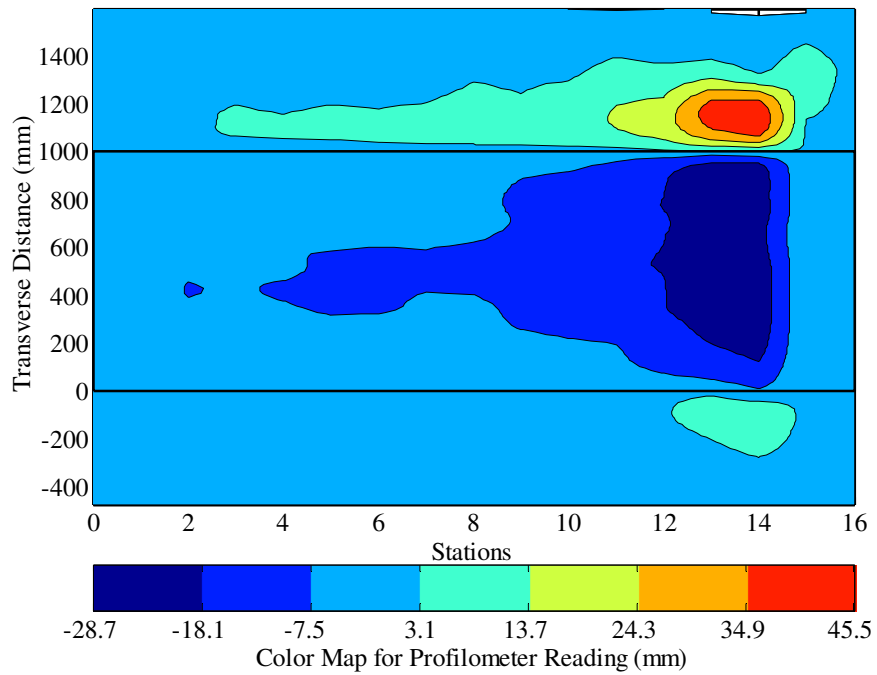


Figure 3.27: Contour plot of permanent deformation after 1,500,000 repetitions.

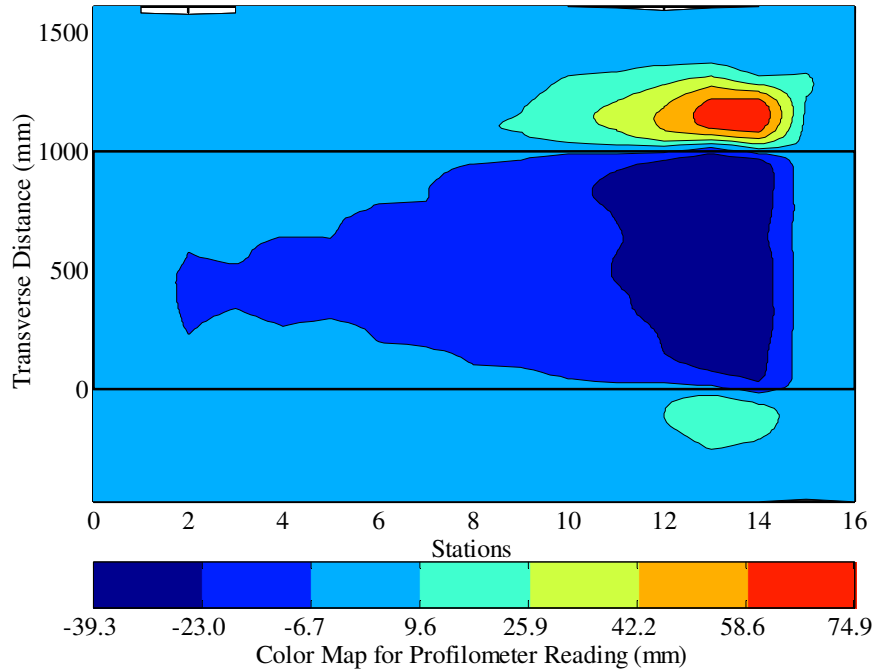


Figure 3.28: Contour plot of permanent deformation at end of test.

After completion of trafficking (2.0 million load repetitions), the average deformation and the average maximum rut depth were 13.1 mm and 37.2 mm respectively. The maximum rut depth measured on the section was 106 mm, at Station 13. The average maximum rut depth exceeded 12.5 mm, the failure criterion determined for the experiment, after about 820,000 repetitions. However, since no cracking was observed on the section at this time, trafficking was continued in an attempt to better understand the performance of the MB4-G overlay. The final surface rutting pattern of the overlay corresponds with the fatigue cracking pattern of the cracked DGAC layer, as shown in Figure 3.29. The deepest rut occurred in the area over the most severe cracking in the underlying layer.

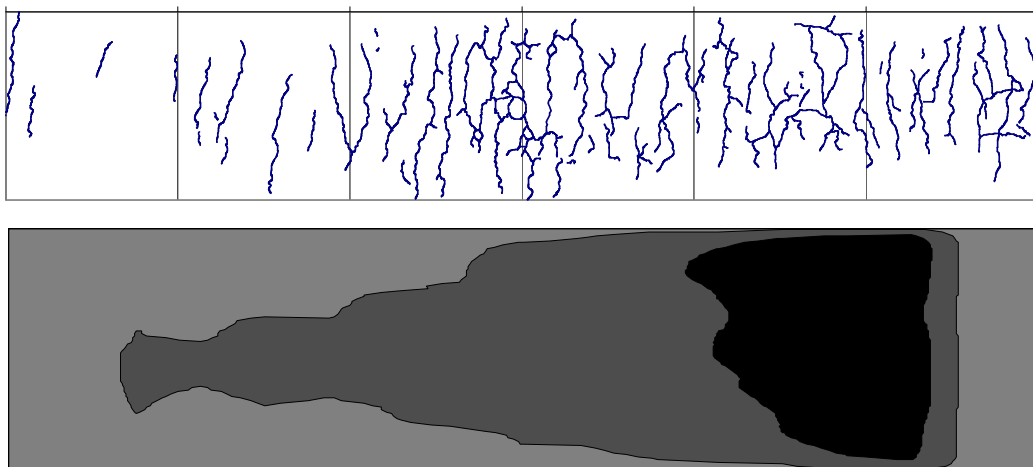


Figure 3.29: Comparison of cracking pattern from Phase 1 and rutting in Phase 2.

3.4.2 Permanent In-depth Deformation

The accumulation of vertical deformation at various depths in the pavement was measured with the MDD linear variable displacement transducer (LVDT) modules during the course of the HVS test. Permanent deformation measured by each LVDT is the total permanent deformation of the pavement between the anchoring depth (3.0 m) and the depth of the module. Accordingly, LVDT modules in the upper part of the pavement typically measure larger permanent deformation than those in the lower part. The difference in measured permanent deformation between two LVDT modules represents the permanent deformation accumulated in the layers between those two modules. This is known as differential permanent deformation. Module locations are shown in Figure 2.6 and are listed below.

- 132 mm: near the bottom of the cracked DGAC layer,
- 337 mm: in the middle of the aggregate base layer
- 542 mm: at the bottom of the aggregate base layer
- 842 mm: 300 mm below the top of the subgrade

A module was not installed on the surface of the RAC-G overlay due to thickness constraints.

Table 3.5 and Figures 3.30 through 3.35 provide an indication of the permanent deformation recorded at MDD4, MDD8, and MDD12 respectively. Figures 3.30, 3.32 and 3.34 show permanent deformation at the MDD modules, while Figures 3.31, 3.33, and 3.35 show the differential deformation calculated for the various layers. The graphs have different scales. Although the MDD data appears to be reliable, firm conclusions about the permanent deformation in the various layers will only be obtained after excavation and assessment of the test pit.

Table 3.5: Vertical Permanent Deformation in Pavement Layers

Layer	Thickness (mm)	Vertical Permanent Deformation (mm)			Percentage Total Deformation (%)		
		MDD4	MDD8	MDD12	MDD4	MDD8	MDD12
After 1,000,000 load repetitions							
AC layers*	135	5.4	7.5	6.9	93.1	92.6	65.7
Aggregate base	410	0.4	0.6	3.1	6.9	7.4	29.5
Subgrade	Semi-infinite	0.0	0.0	0.5	0.0	0.0	4.8
Total (AC+base)		5.8	8.1	10.5	100	100	100
After 2,086,004 load repetitions (test completion)							
AC layers*	135	6.9	11.6	16.7	86.3	75.3	67.9
Aggregate base	410	1.1	3.8	6.3	13.7	24.7	25.6
Subgrade	Semi-infinite	0.0	0.0	1.6	0.0	0.0	6.5
Total (AC+base)		8.0	15.4	24.6	100	100	100
* Laser Profilometer measurement on MDD topcap - top MDD module measurement							

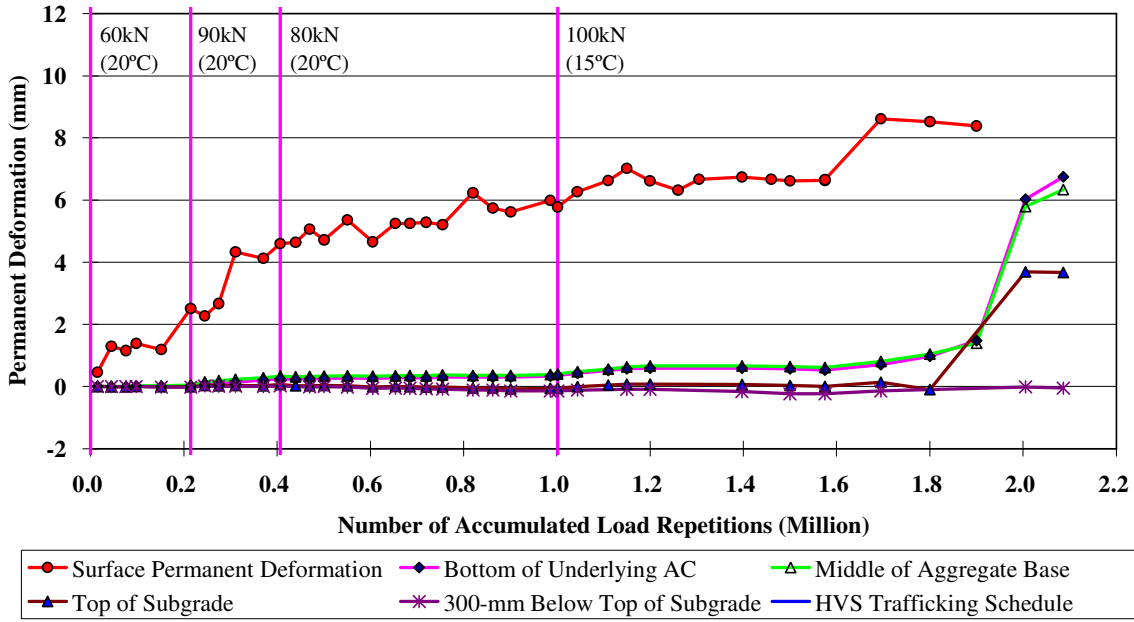


Figure 3.30: In-depth permanent deformation at MDD4.

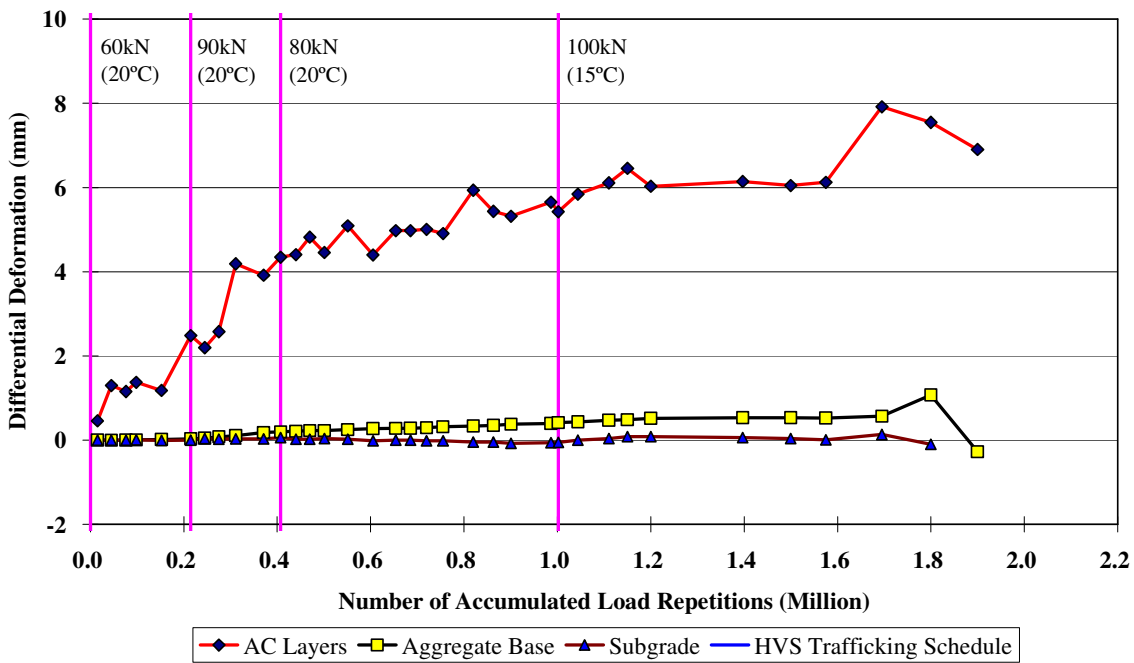


Figure 3.31: In-depth differential permanent deformation of various layers at MDD4.

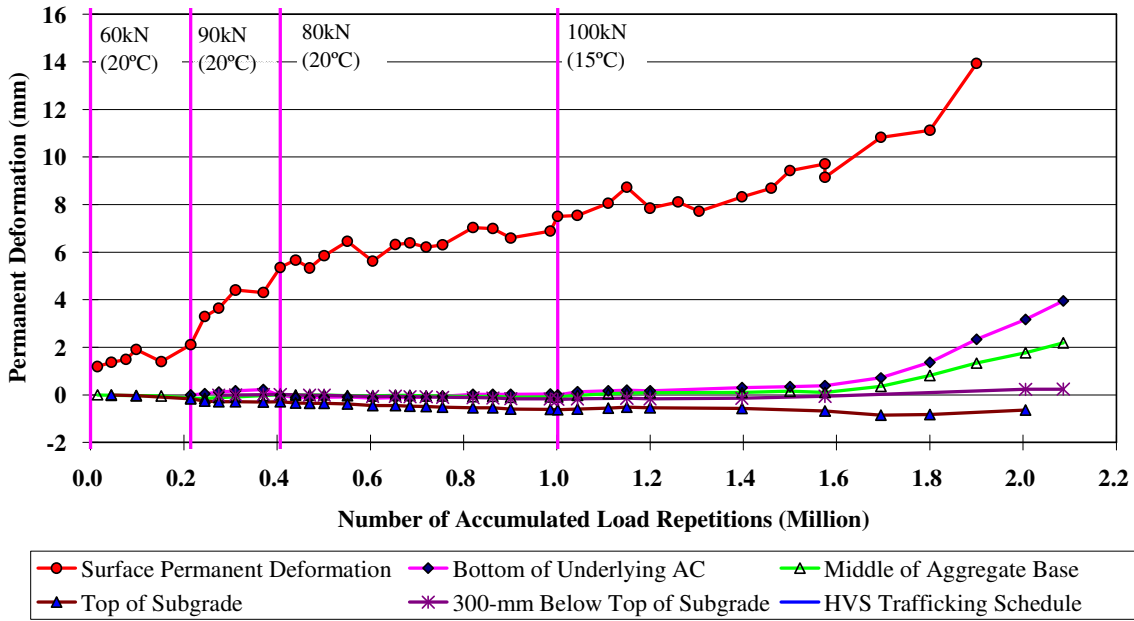


Figure 3.32: In-depth permanent deformation at MDD8.

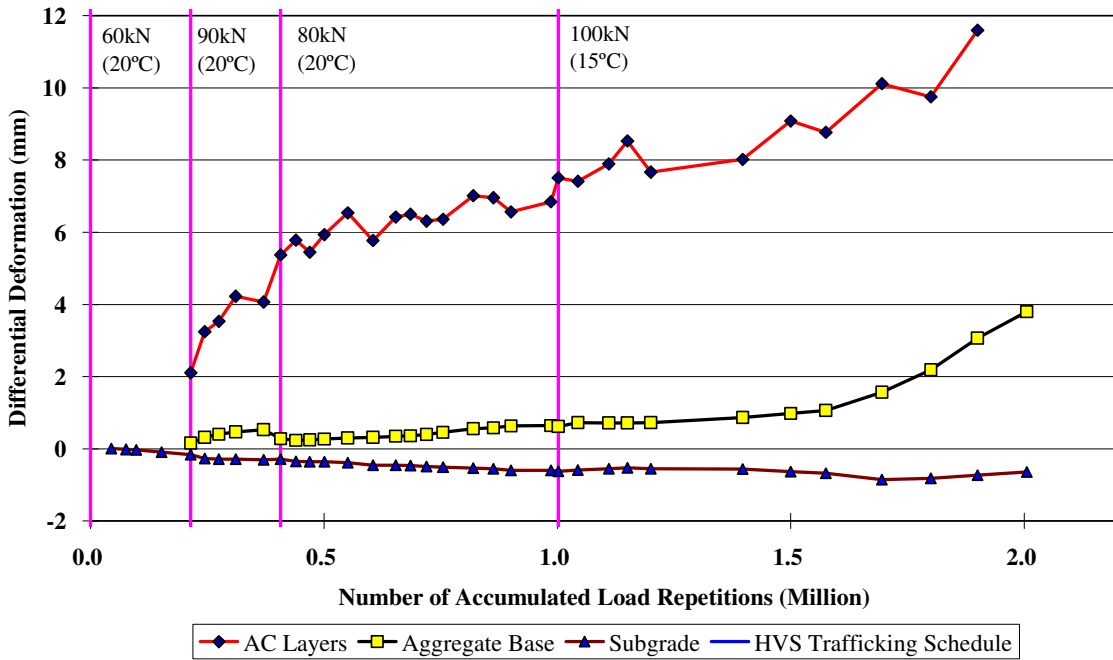


Figure 3.33: In-depth differential permanent deformation of various layers at MDD8.

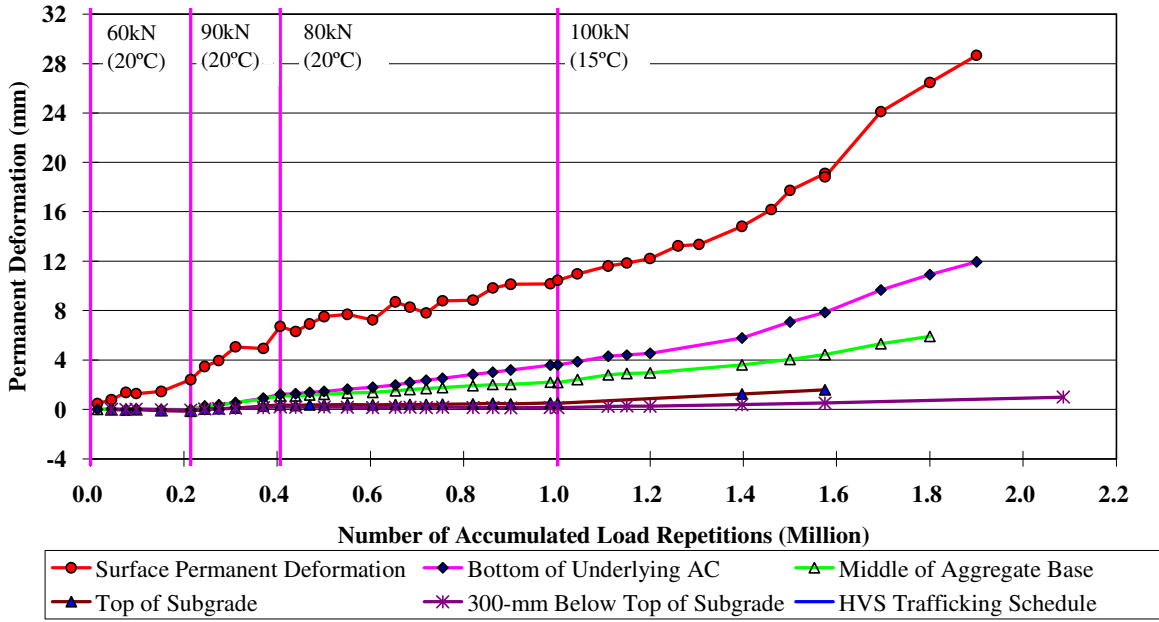


Figure 3.34: In-depth permanent deformation at MDD12.

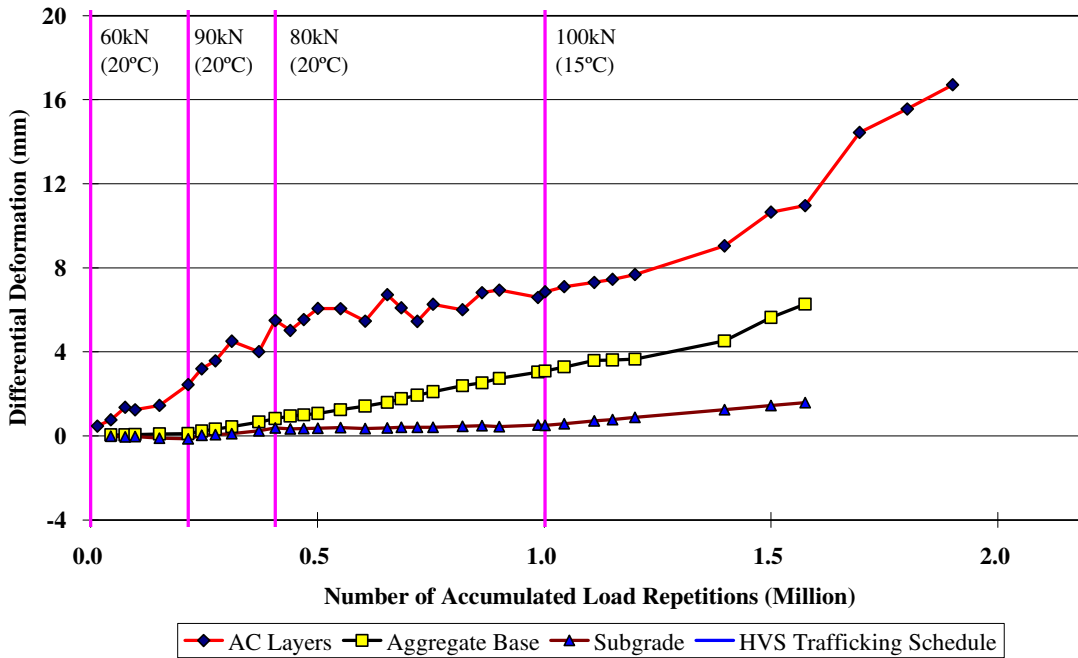


Figure 3.35: In-depth differential permanent deformation of various layers at MDD12.

For the first one million repetitions, most permanent deformation at all of the MDDs occurred in the overlay and cracked DGAC layers, with very little permanent deformation in the aggregate base and in the subgrade. LVDT measurements of permanent deformation at the bottom of the asphalt concrete layers at MDD4 and MDD8 were approximately 0.5 mm and 0.03 mm respectively, while at MDD12 it was

slightly higher at 3.6 mm. In the aggregate base, no permanent deformation was measured at MDD8, while measurements of 0.4 mm and 2.2 mm were recorded at MDD4 and MDD12 respectively.

After the load change, permanent deformation increased at a continuous rate in the surfacing layers (surface deformation measured with the Laser Profilometer minus deformation measured at the 132 mm MDD module) with higher deformation at MDD12 (16.7 mm) where the most severe cracking occurred in the DGAC layer during the first phase of testing. At the end of testing, deformation in the surfacing layers contributed about 86 percent, 75 percent, and 68 percent to the total permanent deformation at MDD4, MDD8, and MDD12 respectively. This indicates that most permanent deformation occurred in the surfacing layers and that more deformation occurred in the surfacing and less in the base where the cracking in the DGAC was less severe (MDD4). In the aggregate base, very little permanent deformation was recorded at MDD4 and at MDD8 until the last few hundred thousand repetitions, with approximately 14 and 25 percent of the total permanent deformation being contributed by this layer at the two stations respectively. At MDD12, permanent deformation increased steadily from the 100 kN load change, with 26 percent of the total permanent deformation being contributed by this layer at this station. Only negligible permanent deformation was recorded in the subgrade at MDD4 and MDD8. However, at MDD12, permanent deformation in the subgrade increased steadily after the 100 kN load change, with deformation in this layer contributing about 6.5 percent to the total recorded at this station.

These trends confirm that the effect of increasing wheel load on permanent deformation diminishes with depth in the pavement structure. The planned forensic investigation will confirm these findings and will be reported on in the second-level analysis report.

3.5. Visual Inspection

Fatigue distress in an asphalt concrete pavement manifests itself in the form of surface cracks. Since this study centered on fatigue cracking and the ability of the overlay to limit reflective cracking from the underlying layer, crack monitoring was an essential component of the data collection program. This entails:

- Visual inspections of the test section and marking of visible cracks,
- Photographic documentation of the marked cracks,
- Correction of the photos for camera angle,
- Digitization of the photos,
- Calculation of the crack length using *Optimas*TM software, and
- Presentation of the cracking in terms of crack length per area of pavement.

Regular crack inspections were made from the time that the first crack was detected through to the end of testing. The first cracks appeared between Stations 12 and 14 after about 1.5 million repetitions and were considered to be associated with the permanent deformation (rutting and shoving) discussed in the previous section. Cracks continued to appear for a short period until about 1.6 million repetitions, after which no further cracking was noted. The observed cracks were less than 1.0 mm wide and difficult to detect visually. They did not spall or increase in width during testing. Most cracking was longitudinal and did not mirror the cracking in the underlying layer. At the end of testing, 29 cracks were identified with a total length of 4.51 m and an average spacing of 200 mm. This equates to a crack density of 1.55 m/m², considerably lower than the failure criterion of 2.5 m/m² set for the experiment. Figure 3.36 shows the surface between Stations 12 and 14 at the end of testing, with cracks highlighted. The deformation is also clearly visible.



Figure 3.36: Surface cracks marked with crayon between Stations 12 and 14 at end of test.

Figure 3.37 shows a schematic of the cracking on Section 589RF and a comparison of the cracking with that on the underlying Section 571RF. The figure clearly shows that the cracking is limited to one end of the section and that the patterns do not correspond. Apart from the cracks associated with deformation at the end of the section, the MB4-G overlay appeared to successfully prevent any cracking in the underlying layer from reflecting through to the surface. This is interesting, considering that the calculated ratios of final-to-initial deflections indicate considerable damage occurred in the asphalt layers.

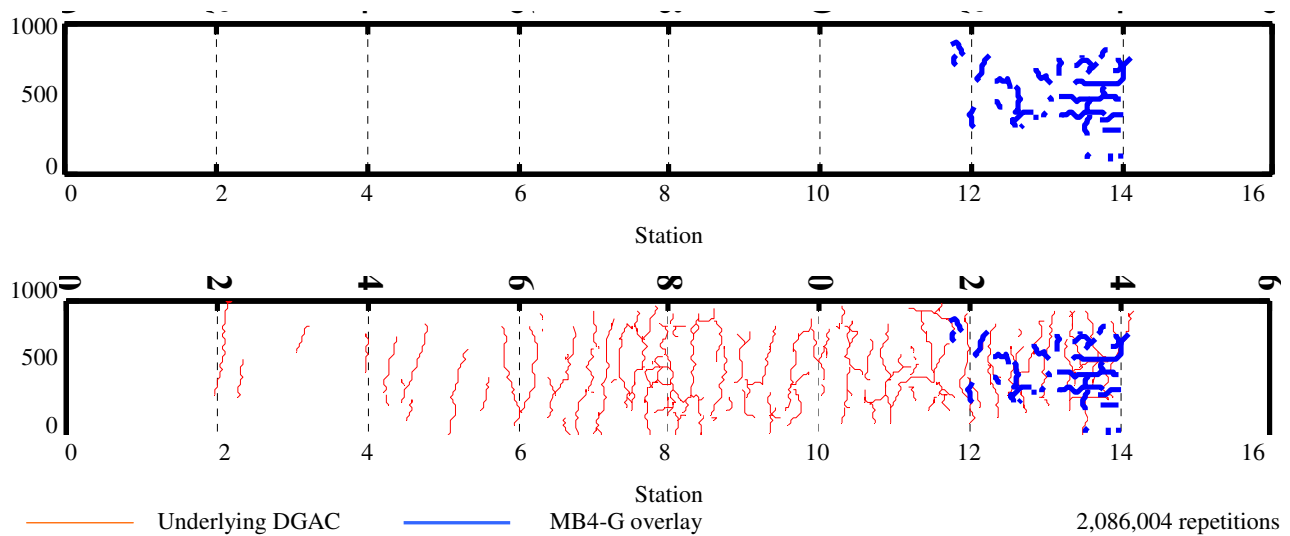


Figure 3.37: Cracking pattern and pattern comparison between underlying layer and overlay.

3.6. Forensic Evaluation

A forensic evaluation (coring and test pit) can only be undertaken when HVS testing all of the six sections has been completed. Results of the forensic evaluation will be discussed in a second-level analysis report on completion of the tests.

3.7. Second-level Analysis

A second-level analysis report will be prepared on completion of all HVS testing and a forensic evaluation. This report will include:

- Actual layer thicknesses,
- Backcalculation of moduli from RSD, MDD, and FWD measurements,
- Verification of data collected from in-depth measurements with visual observations from test pits,
- Comparison of performance between test sections,
- Comparisons of HVS test results with laboratory test results, and
- Recommendations.

4. CONCLUSIONS

This First-level Report is the second in a series of studies detailing the results of HVS testing being performed to validate Caltrans overlay strategies for the rehabilitation of cracked asphalt concrete. It describes the results of the second HVS reflective cracking testing section (589RF) carried out on a 45-mm (1.7 in) half-thickness MB4-G overlay. Other overlays that will be tested during the course of the experiment include:

- Full-thickness (90 mm) MB4 gap-graded overlay (90 mm MB4-G);
- Half-thickness (45 mm) MB4 gap-graded overlay with minimum 15 percent recycled tire rubber (MB15-G);
- Half-thickness MAC15TR gap-graded overlay with minimum 15 percent recycled tire rubber (MAC15-G);
- Half-thickness rubberized asphalt concrete gap graded overlay (RAC-G) overlay, included as a control for performance comparison purposes, and
- Full-thickness (90 mm) AR4000-D overlay, included as a control for performance comparison purposes

The pavement was designed according to the Caltrans Highway Design Manual Chapter 600 using the computer program *NEWCON90*. Design thickness was based on a subgrade R-value of 5 and a Traffic Index of 7 (~121,000 ESALs). The overlay thickness was determined according to Caltrans Test Method (CTM) 356 using Falling Weight Deflectometer (FWD) deflections.

HVS trafficking on the section commenced on June 23, 2004, and was completed on February 8, 2005. A temperature chamber was used to maintain the pavement temperature at $20^{\circ}\text{C}\pm 4^{\circ}\text{C}$ for the first one million repetitions, then at $15^{\circ}\text{C}\pm 4^{\circ}\text{C}$ for the remainder of the test. During this period a total of 2,086,004 load repetitions (tire pressure of 720 kPa [104 psi], and bi-directional trafficking pattern with wander) were applied, consisting of:

- 215,000 repetitions of a 60 kN (13,500 lb) load,
- 192,197 repetitions of a 90 kN (20,250 lb) load,
- 594,803 repetitions of an 80 kN (18,000 lb) load, and
- 1,084,004 repetitions of a 100 kN (22,500 lb) load.

This loading equates to approximately 68.7 million equivalent standard axles, using the Caltrans conversion of $(\text{axle load}/18000)^{4.2}$, which in turn equates to a Traffic Index of 15.

Testing was interrupted during a breakdown between October 13 and November 29, 2004, when the cumulative traffic repetitions were approximately 1.2 million, and for the scheduled holiday shutdown between December 24, 2004, and January 04, 2005, when the repetition count was 1,575,000.

Laboratory fatigue and shear studies have been conducted in parallel with HVS testing. Results of these studies will be detailed in separate reports. Comparison of the laboratory and test section performance, including the results of a forensic investigation to be conducted when all testing is complete, will be discussed in a second-level report once the data from each of the studies have been collected.

Findings and observations based on the data collected during this HVS study include:

- Cracking was observed at one end of the section where significant deformation (rutting and shoving) had occurred. It was first recorded after 1.5 million repetitions and no further cracking was noted after about 1.6 million repetitions. On completion of testing, the crack density was 1.55 m/m^2 (0.47 ft/ft^2), considerably lower than the failure criterion of 2.5 m/m^2 (0.76 ft/ft^2) set for the experiment. The cracks were predominantly longitudinal and cracking patterns did not correspond with those in the underlying DGAC layer. Apart from the cracks associated with deformation at the end of the section, the MB4-G overlay appeared to successfully prevent any cracking in the underlying layer from reflecting through to the surface, despite final-to-initial deflections indicating that considerable damage had occurred in the asphalt layers.
- The average maximum rut depth across the entire test section at the end of the test was 37.2 mm (1.46 in) which exceeded the Caltrans (and experiment) failure criterion of 12.5 mm (0.5 in) reached after approximately 820,000 repetitions. At this point, no cracking was observed and the test was therefore continued to gain a better understanding of the MB4-G overlay performance. The maximum rut depth measured on the section was 106 mm (4.17 in). Despite conducting HVS testing at relatively low pavement temperatures ($20^\circ\text{C}\pm 4^\circ\text{C}$ [$68^\circ\text{F}\pm 7^\circ\text{F}$] for the first one million repetitions and $15^\circ\text{C}\pm 4^\circ\text{C}$ [$59^\circ\text{F}\pm 7^\circ\text{F}$] for the remainder of the test), the MB4-G overlay appeared susceptible to rutting from early in the experiment.
- Ratios of final-to-initial elastic surface deflections under a 60 kN (13,500 lb) wheel load increased by between 2.1 and 2.9 times along the length of the section. The ratios for in-depth deflections show that damage had increased significantly at all depths in the pavement structure by the end of trafficking. Loss of stiffness was highest in the area of most severe cracking in the underlying DGAC layer.
- Analysis of surface profile and in-depth permanent deformation measurements indicate that most of the permanent deformation (between 68 and 86 percent along the length of the section) occurred in the asphalt-bound surfacing layers (overlay and cracked DGAC) with the remainder in

the aggregate base layer. Some deformation occurred in the subgrade below the point of greatest maximum rut. Contribution to total permanent deformation at this point was 68, 26, and 6 percent for the surfacing, aggregate base, and subgrade respectively.

No recommendations as to the use of MB4-G mixes are made at this time. These recommendations will be included in the second-level analysis report, which will be prepared and submitted on completion of all HVS and laboratory testing.

5. REFERENCES

1. **Generic experimental design for product/strategy evaluation — crumb rubber modified materials.** 2005. Sacramento, CA: Caltrans.
2. **Reflective Cracking Study: Workplan for the Comparison of MB, RAC-G, and DGAC Mixes Under HVS and Laboratory Testing.** 2003. Davis and Berkeley, CA: University of California Pavement Research Center. (UCPRC-WP-2003-01).
3. BEJARANO, M., Jones, D., Morton, B., and Scheffy, C. 2005. **Reflective Cracking Study: Summary of Construction Activities, Phase 1 HVS Testing, and Overlay Construction.** Davis and Berkeley, CA: University of California Pavement Research Center. (UCPRC-RR-2005-03).
4. HARVEY, J., Du Plessis, L., Long, F., Deacon, J., Guada, I., Hung, D. and Scheffy, C. 1997. **CAL/APT Program: Test Results from Accelerated Pavement Test on Pavement Structure Containing Asphalt Treated Permeable Base (ATPB) – Section 500RF.** Davis and Berkeley, CA: University of California Pavement Research Center. (Report Numbers UCPRC-RR-1999-02 and RTA-65W4845-3).
5. HARVEY, J., Du Plessis, L., Long, F., Deacon, J., Guada, I., Hung, D. and Scheffy, C. 1997. **CAL/APT Program: Test Results from Accelerated Pavement Test on Pavement Structure Containing Untreated Base – Section 501RF.** Davis and Berkeley, CA: University of California Pavement Research Center. (Report Numbers UCPRC-RR-1997-03 and RTA-65W4845-3).

